Plastoquinol generates and scavenges reactive oxygen species in organic solvent: potential relevance for thylakoids

Sergey Khorobrykh and Esa Tyystjärvi*

Department of Biochemistry/Molecular Plant Biology, University of Turku, FI-20014 Turku, Finland.

Abstract

The present work reports reactions of plastoquinol (PQH_2-9) and plastoquinone (PQ-9) in organic solvents and summarizes the literature to understand similar reactions in thylakoids. In thylakoids, PQH_2-9 is oxidized by the cytochrome b_6/f complex (Cyt b_6/f) but some PQH_2-9 is also oxidized by reactions in which oxygen acts as an electron acceptor and is converted to reactive oxygen species (ROS). Furthermore, PQH_2-9 reacts with ROS. Light enhances oxygen-dependent oxidation of PQH_2-9. We examined the oxidation of PQH_2-9 via dismutation of PQH_2-9 and PQ-9 and scavenging of the superoxide anion radical ($O_2^{\bullet-}$) and hydrogen peroxide (H_2O_2) by PQH_2-9. Oxidation of PQH_2-9 via dismutation to semiquinone was slow and independent of pH in organic solvents and in solvent/buffer systems, suggesting that intramembraneous oxidation of PQH_2-9 in darkness mainly proceeds via reactions catalyzed by the plastid terminal oxidase and cytochrome b_{559}. In the light, oxidation of PQH_2-9 by singlet oxygen and by $O_2^{\bullet-}$ formed in PSI contribute significantly. In addition, Cyt b_6/f forms H_2O_2 with a PQH_2-9 dependent mechanism. Measurements of the reaction of $O_2^{\bullet-}$ with PQH_2-9 and PQ-9 in acetonitrile showed that $O_2^{\bullet-}$ oxidizes PQH_2-9, forming PQ-9 and several PQ-9-derived products. The rate constant of the reaction between PQH_2-9 and $O_2^{\bullet-}$ was found to be 10^4 M^{-1} s^{-1}. H_2O_2 was found to oxidize PQH_2-9 to PQ-9, but failed to oxidize all PQH_2-9, suggesting that the oxidation of PQH_2-9 by H_2O_2 proceeds via deprotonation mechanisms producing PQH^--9, PQ^{2-}-9 and the protonated hydrogen peroxide cation, $H_3O_2^+$.

Keywords: Hydrogen peroxide, plastoquinone, singlet oxygen. superoxide anion radical, thylakoid membrane.

Abbreviations: Chl, chlorophyll; Cyt b_{559}, cytochrome b_{559}; Cyt b_6/f, cytochrome b_6/f complex; DMSO, dimethylsulfoxide; DNP-INT, 2-iodo-6-isopropyl-3-methyl-2',4,4'-trinitrodiphenyl ether; DCMU, 3-(3,4-Dichlorophenyl)-1,1-dimethylurea; HEPES, 4-(2-hydroxyethyl)-1-piperazineethanesulfonic acid; $HO_2^{\bullet}$, hydroperoxyl radical; HPLC, high performance liquid chromatography; MeOH, methanol; MES, 2-(N-morpholino)ethanesulfonic acid; $^1O_2$, singlet oxygen; $O_2^{\bullet-}$, superoxide anion radical; P_{680}, primary electron donor of PSII; $PQH^{\bullet}$-9 and $PQ^{\bullet-}$-9 , plastosemiquinone radical and plastosemiquinone anion radical, respectively; PQH_2-9 and PQ-9, plastoquinol and

plastoquinone, respectively; PSI and PSII, photosystems I and II, respectively; PTOX, plastid terminal oxidase; ROS, reactive oxygen species;

*Author for correspondence. E-mail esatyy@utu.fi, Tel. +358405113503.

1. Introduction

Photosynthetic electron transport in plants, algae and cyanobacteria contributes to conversion of light energy to energy of chemical bonds. Light absorbed by the chlorophyll (Chl) molecules of Photosystems I and II (PSI and PSII) triggers a sequence of redox reactions along the thylakoid membrane. These reactions result in oxidation of water, reduction of $NADP^+$ to NADPH and formation of a proton gradient across the thylakoid membrane. In addition to the linear electron transport, both PSI and PSII mediate cyclic electron flow, a plastid terminal oxidase mediates chlororespiration, and both photosystems mediate electron flow known as the water-water cycle, part of which is the Mehler-peroxidase reaction (MPR) [1-3].

In the chloroplast, oxygen can be converted to reactive oxygen species (ROS) like singlet oxygen ($^1O_2$), superoxide anion radical ($O_2^{\bullet-}$) and hydrogen peroxide (H_2O_2). ROS are considered unfavorable for chloroplast functions because ROS may damage biomolecules. Chloroplasts have ROS scavenging systems that diminish the damage [4]. On the other hand, ROS also play important roles in plant signaling and acclimation [5-7]. In particular, formation of ROS in Mehler's reaction initiates ascorbate and glutathione dependent light signaling [8].

The highly reactive $^1O_2$ is mainly formed through a reaction of the triplet excited state of chlorophyll (^{3}Chl*) and the ground state of molecular oxygen, $^3O_2$. The main site of $^1O_2$ generation is the reaction center of PSII where the triplet state of the primary donor, $^3P_{680}$, is formed by charge recombination reactions between P_{680}^+, tyrosine Z^+ or states S2 or S3 of the oxygen evolving complex, and Q_A^- or Q_B^- the primary and secondary quinone acceptors of PSII [9, 10]. In plants, $^1O_2$ is mainly quenched by carotenoids, as the second-order rate constants of the reaction of $^1O_2$ with carotenoids are in the range of 7×10^9 to 1.4×10^{10} M^{-1} [11]. In addition, plastoquinone and tocopherols can efficiently scavenge $^1O_2$ inside the thylakoid membrane, as both react rapidly with $^1O_2$ with rate constants in the range of 10^7 to 10^8 M^{-1} s^{-1} [12] and both are abundant in the thylakoid membrane [13].

ROS-dependent photochemical quenching of light energy is mostly associated with MPR. In plants and algae, MPR operates in the chloroplast stroma and consists of ROS

production (Mehler's reaction), scavenging of ROS, and regeneration of the scavenging system [14]. MPR starts with the formation of $O_2^{\bullet-}$ on the acceptor side of PSI via one-electron reduction of oxygen by the terminal acceptors F_X, F_A, and F_B of PSI [15]. In isolated thylakoid membranes, the maximum rate of PSI-dependent production of $O_2^{\bullet-}$, obtainable in high light, was estimated to be 15–20 μmol of $O_2^{\bullet-}$ (mg Chl)$^{-1}$ h^{-1} [14, 16] or 7.5–10 μmol of H_2O_2 (mg Chl)$^{-1}$ h^{-1} if all $O_2^{\bullet-}$ are converted to H_2O_2 via the superoxide dismutation reaction.

In isolated thylakoid membranes, Mehler's reaction is fully suppressed if electron transfer from PSII to PSI is inhibited by DCMU that blocks electron transfer from PSII to the plastoquinone (PQ) pool. However, the rate of H_2O_2 production by isolated thylakoids in the light decreased only marginally when electron transfer from PSII to PSI was suppressed by 2,4-dinitrophenylether of iodonitrothymol (DNP-INT) that inhibits the oxidation of PQH_2-9 by the cytochrome *b*$_6$*f* complex (Cyt *b*$_6$*f*) [17]. Thus, the maximum rate of O_2 reduction via PQ pool dependent mechanism(s) was estimated to be 20 μmol H_2O_2 (mg Chl)$^{-1}$ h-^{1} [17].

It was recently found that Cyt *b*$_6$*f* can oxidize PQH_2-9 in a reaction that produces $O_2^{\bullet-}$ and H_2O_2 [18]. PQH_2-9 can also be oxidized by plastid terminal oxidase (PTOX) with formation of PQH_2-9 and H_2O as final products of the reaction [19, 20]. It has also been reported that $O_2^{\bullet-}$ and H_2O_2 can be generated via oxidation of PQH_2-9 by PTOX [21]. The maximum rate of oxidation of PQH_2-9 by PTOX in higher plants, observed when the plastoquinone pool is fully reduced, is 0.15-0.2 PQH_2-9 PSII^{-1} s^{-1} [19, 20, 22], or 1.4-1.9 μmol PQH_2-9 (mg Chl)$^{-1}$ s^{-1}, if the Chl to PSII ratio is 420. $O_2^{\bullet-}$ can also be formed via reduction of O_2 by reduced phaeophytin *a* and the semiquinone form of the electron acceptor Q_A of PSII [23, 24].

In summary, the reduction of O_2 associated with formation of ROS can be proceeded via six mechanisms in the thylakoid membrane. (i) Dismutation of PQH_2-9 and PQ-9 can produce the plastosemiquinone anion radical $PQ^{\bullet-}$-9 that would reduce O_2 to $O_2^{\bullet-}$. (ii) The low-potential form of cytochrome *b*$_{559}$ (Cyt *b*$_{559}$) can both reduce O_2 to $O_2^{\bullet-}$ [25] and catalyze the reduction of O_2 by PQH_2-9 [26, 27]. (iii) Phylloquinone A_1, a secondary electron acceptor in PSI, may reduce O_2 to $O_2^{\bullet-}$ [28, 29]. In the fourth mechanism (iv), oxidation of PQH_2-9 by $^1O_2$ [30-33] produces H_2O_2 [34]. Furthermore, $O_2^{\bullet-}$ (or its protonated form $HO_2^{\bullet}$) formed by mechanisms (i-iii) can be reduced to H_2O_2 within the membrane by PQH_2-9 [16, 17, 29, 35] or by Cyt *b*$_{559}$. (v) H_2O_2 can be formed in association with oxidation of PQH_2-9 by Cyt *b*$_6$*f* [18]. (iv) $O_2^{\bullet-}$ and H_2O_2 can be formed in PTOX-mediated oxygen reduction [21]. There is no information about scavenging of H_2O_2 inside the thylakoid membrane.

The above data show that PQH_2-9 can both produce and scavenge reactive oxygen species (ROS) within the thylakoid membrane. However, it was not clear which reactions between PQH_2-9 and oxygen are most effective in oxidizing PQH_2-9. In the present work we studied the rates and products of the reactions of $O_2^{\bullet-}$ and H_2O_2 with PQH_2-9 in organic solvents. Acetonitrile was selected for reactions of $O_2^{\bullet-}$ because $O_2^{\bullet-}$ cannot be protonated in it. In addition, methanol (a water miscible solvent) was compared to hexane (a water immiscible solvent). Furthermore, methanol solutions buffered to different pH values were used to study the effects of protons on autoxidation of plastoquinol in the presence of plastoquinone. The results show that $O_2^{\bullet-}$ and H_2O_2 can oxidize PQH_2-9 to PQ-9. The present work analyses the results in the light of literature about the reactions of quinones with ROS and about participation of thylakoid protein complexes on these reactions, and significant ROS-dependent oxidation of the PQ-pool is suggested.

2. Materials and Methods

2.2. Isolation of thylakoids

Thylakoid membranes were isolated from pumpkin (*Cucurbita maxima* L.) leaves as described in [16] with some modifications. Leaves were ground in buffer (40 mM HEPES-KOH, pH 7.4, 330 mM sorbitol, 0.5 mM $MnCl_2$, 0.5 mM $MgCl_2$, 1 mM ethylenediamine tetraacetic acid, 1% bovine serum albumin) in 20-s cycles for 1 min at 4 °C. The suspension was centrifuged for 5 min at 1500×g and the pellet was suspended in osmotic shock buffer (10 mM HEPES, pH 7.4, 5 mM sorbitol and 5 mM $MgCl_2$). The suspension was again centrifuged for 5 min at 1500×g and the pellet was suspended in storage buffer containing 10 mM HEPES (pH 7.4), 330 mM sorbitol, 4 mM $MgCl_2$, 10 mM NaCl, and 20% glycerol.

2.2. Purification of plastoquinone

PQ-9 was isolated from pumpkin thylakoid membranes on a preparative scale using an alumina column-based method [36]. After extraction with an alumina column, PQ was purified using a high performance liquid chromatography (HPLC) based method [37] with some modifications. Briefly, the HPLC purification was performed with LiChroCART (Germany) C_{18} reversed-phase column (LiChrospher 100, 125 × 4 mm, 5 μm) using an Agilent 1100 series device with absorption and fluorescence detectors (Agilent Technologies, Palo Alto, CA), and using an isocratic solvent system (methanol:hexane, 34:2 v:v). The flow rate was 0.75 ml/min, the temperature of the column was maintained at 25 °C, and the

injection volume was 40 µl. PQ-9 was detected with absorption at 255 nm. Pure PQ-9 was collected according to the retention times of the corresponding peaks on the chromatogram using Analyt-FC (Agilent Technologies, Palo Alto, CA) collector. Finally, the pure PQ-9 in methanol/hexane was dried under N_2 stream and dissolved with acetonitrile. PQH_2-9 was prepared by reducing pure PQ-9 by $NaBH_4$ in (acetonitrile:water, 5:1 v:v) solution. PQH_2-9 was extracted by hexane to remove $NaBH_4$. The pure PQH_2-9 in hexane was dried under N_2 stream and dissolved in acetonitrile or methanol, as indicated. PQH_2-9 was measured with fluorescence excitation/emission detection at 290/330 nm.

2.3. Detection of PQ-derived compounds and preparation of samples

The same HPLC-based method as described above for purification of PQ-9 was applied to detection of PQ-derived compounds, except that the isocratic solvent system (methanol:hexane, 34:2) was replaced with methanol. To study autoxidation of PQH_2-9, mixtures of PQH_2-9/PQ-9 were prepared in methanol. The autoxidation of PQH_2-9 was measured, as indicated, in methanol, in methanol:H_2O mixture (1:1) and in methanol:buffer mixture (1:1) to which HEPES-KOH, pH 8.0 and MES-KOH, pH 5.0 were added to adjust the pH. The samples were incubated for 0, 35, 70 and 105 min at 25 °C and analyzed with HPLC. To measure autoxidation of PQH_2-9 in hexane, mixture of PQH_2-9/PQ-9 in methanol was dried under N_2 flow and dissolved in hexane. The autoxidation of PQH_2-9 in hexane was also measured in a two-phase system prepared by adding an equal volume of water or one of the buffers as described above, to a mixture of PQH_2-9/PQ-9 in hexane. To analyze the PQ-derived compounds in hexane, 50 µl of the hexane fraction was dissolved in 200 µl of methanol and immediately analyzed with HPLC.

The reaction of KOH with PQH_2-9 or PQ-9 was studied in methanol. 5 µl of KOH in aqueous solution was added to 60 µl of PQH_2-9 or PQ-9 solution, incubated for 2 min at 25 °C in the dark and then used for HPLC analysis. Reactions of H_2O_2 with PQH_2-9, PQ-9 or PQH_2-9/PQ-9 mixture were studied in methanol. 5 µl of H_2O_2 in aqueous solution was added to 60 µl of PQ-9 or PQH_2-9/PQ-9 solution in methanol, incubated for 2 and 40 minutes at 25 °C in the dark and then used for HPLC analysis. Reaction of $O_2^{\bullet-}$ with PQH_2-9 and PQ-9 was carried out by addition of 10 µl of KO_2 in dimethylsulfoxide (DMSO) to 60 µl of PQH_2-9 or PQ-9 solutions in acetonitrile. The samples were incubated for 2 min in the dark at 25 °C and then analyzed with HPLC.

2.4. Preparation of $O_2^{\bullet-}$ solution

Solution of $O_2^{\bullet-}$ was prepared by dissolving KO_2 with DMSO in the presence of 18-Crown-6 (1,4,7,10,13,16-hexaoxacyclooctadecane). The concentration of $O_2^{\bullet-}$ was measured

with oxygen evolution after addition of KO_2 solution to the buffer containing 50 mM Mes-KOH, pH 5.0 using a Clark-type oxygen electrode. Concentration of $O_2^{\bullet-}$ was calculated from the stoichiometry between $O_2^{\bullet-}$ and oxygen evolution according to Reaction 1 [38].

$$2KO_2 + 2H_2O = 2KOH + H_2O_2 + O_2 \quad (1)$$

2.5. Determination of the second order rate constant of the reaction between $O_2^{\bullet-}$ and PQH_2-9

Rapid kinetic measurements were performed with an Applied Photophysics (Leatherhead, UK) SX.18MV stopped-flow instrument at 25 °C. Prior to loading the samples, the instrument was carefully washed with dried DMSO ($O_2^{\bullet-}$ side) and acetonitrile (PQH_2-9 side) in order to remove water. The reactions were initiated by mixing 60 µl of 250 µM PQH_2-9 in acetonitrile with 60 µl of 1-20 mM $O_2^{\bullet-}$ in DMSO. PQH_2-9 was excited at 290 nm and emitted light was collected through a 320 nm long-pass filter. At least three individual traces were averaged for each reported curve.

2.6. Detection of H_2O_2

H_2O_2 was measured with chemiluminescence of the luminol-H_2O_2-horseradish peroxidase system. The reaction medium (330 µl) contained 2.5 mM luminol, 10 mM Tris-HCl buffer at pH 8.4, and 10 U/ml horseradish peroxidase. The solution was continuously stirred with a magnetic bar. The chemiluminescence reaction was triggered by manual injection of 20 µl of sample. Due to enhancement of chemiluminescence by PQH_2-9, the ratio of chemiluminescence intensity to H_2O_2 concentration depends on the concentration of PQH_2-9 [34]. For precise measurement of H_2O_2, the samples were after the reaction diluted by 400 times in H_2O and divided to two parts. Aqueous solution of H_2O_2 (final concentration 12.5 µM) was added to one part and an equal volume of H_2O was added to the other part. The amount of H_2O_2 was then calculated according to the equation H_2O_2 (µM) = $a/(b-a)$, where a and b are the intensity of the chemiluminescence in the absence and presence of 12.5 µM H_2O_2, respectively. The chemiluminescence measurements were carried out using an EMI9558B photon multiplier tube using a set-up earlier designed for thermoluminescence measurements [39].

3. Results

3.1. Autoxidation of PQH_2-9 is very slow in physiological pH

It has been suggested that autoxidation of PQH_2-9 by oxygen in thylakoid membranes could be related to formation of $PQH^{\bullet}$-9 via a dismutation reaction (Reaction 2)

$$PQH_2\text{-}9 + PQ\text{-}9 \leftrightarrows 2PQH^{\bullet}\text{-}9 \quad (2)$$

followed by deprotonation of $PQH^{\bullet}$-9 (Reaction 3) and oxidation of $PQ^{\bullet-}$-9 by O_2 (Reaction 4) [17].

$$2PQH^{\bullet}\text{-}9 \leftrightarrows PQ^{\bullet-}\text{-}9 + 2H^{+} \quad (3)$$

$$PQ^{\bullet-}\text{-}9 + O_2 \leftrightarrows PQ\text{-}9 + O_2^{\bullet-} \quad (4)$$

To estimate the significance of Reactions 2-4, the oxidation of PQH_2-9 was measured in a mixture of PQH_2-9/PQ-9 in both polar and nonpolar organic solvents, methanol (water miscible organic solvent) and hexane (water immiscible organic solvent) respectively. We used methanol and hexane on purpose to check the influence of oxidation of a mixture of PQH_2-9/PQ-9 in different organic solvents. In addition, we used buffers with different pH values to study the effect of protons on autoxidation of plastoquinol in the presence of plastoquinone. The samples were analyzed with HPLC immediately after incubation. As shown in Fig. 1 (A, D), oxidation of PQH_2-9 in pure methanol or hexane is very slow. As the oxygen concentrations in methanol and hexane are 2.42 mM and 3.58 mM, respectively [40], the respective rate constants of PQH_2-9 oxidation in methanol and hexane were 7.85×10^{-3} M^{-1} s^{-1} and 4.71×10^{-3} M^{-1} s^{-1} (Table 1). These results are in accordance with earlier data [26].

The oxidation of PQH_2-9 in aqueous solutions can mostly occur via reaction of O_2 with one of the deprotonated forms of PQH_2-9, PQH^{-}-9 or PQ^{2-}-9, and Reaction 4. Thus, oxidation of PQH_2-9 should be pH dependent due to the pH-dependence of the redox potentials of PQ-9/$PQH^{\bullet}$-9, PQH_2-9/$PQH^{\bullet}$-9 and $O_2/O_2^{\bullet-}$ [41, 42]. At physiological pH, the autoxidation of PQH_2-9 is rather slow because the pK_1 and pK_2 values for PQH_2-9 are near to the pK values of tetramethyl-*p*-benzoquinone, 10.8 and 12.9, respectively [43] and the redox potential of PQH_2-9/$PQH^{\bullet}$-9 is 385 mV at pH 7.0 [42] which is much positive than the redox potential of $O_2/O_2^{\bullet-}$ (-160 mV) [14]. Efficient autoxidation of PQH_2-9 can be observed only at high pH. The redox potential of PQ-9/$PQH^{\bullet}$-9 becomes lower (-170 mV) above pH 6.0 when $PQH^{\bullet}$-9 is mostly deprotonated. Thus, in physiological pH, autoxidation of PQH_2-9 should occur via Reaction 4

To test the influence of the physiological pH range on PQH_2-9 oxidation, 50 mM Mes-KOH (pH 5.0) and 50 mM Hepes-KOH (pH 8.0) were added to a mixture of PQH_2-9/PQ-9 in both methanol and hexane. In the case of the hexane solution, the oxidation of PQH_2-9/PQ-9 may occur both in the hexane phase and at the hexane/buffer interface. The

autoxidation of PQH_2-9 in both methanol/buffer and hexane/buffer systems was slow and independent of pH (Fig. 1 C, D and F, E). Because the oxygen concentration of the methanol/buffer system is approximately 471 µM [44], the second order rate constant of PQH_2-9 oxidation in the methanol/buffer system was 2.9×10^{-2} M^{-1} s^{-1}. Assuming that the oxidation of PQH_2-9 occurred at the interface of the hexane/buffer system where the oxygen concentration would be the same as in the aqueous solution, 253 µM, the second order rate constant was 1.8×10^{-2} M^{-1} s^{-1} (Table 1). A low rate constant for the oxidation of PQH_2-9 has also been measured in a liposome-buffer system at pH 7.8 [26]. Assuming that oxidation of PQH_2-9 in both methanol/buffer and at the hexane/buffer interface can be considered similar to oxidation of PQH_2-9 in aqueous phase, the pH-independence of PQH_2-9 oxidation indicates that the formation of $PQH^{\bullet}$-9 is highly unfavorable. The equilibrium constant K_s for Reaction 2, calculated from the equation $E(mV) = 60\times\log K_s$ where $E = E(PQH^{\bullet}\text{-}1/\ PQ\text{-}1) - E(PQH_2\text{-}1/\ PQH^{\bullet}\text{-}1)$ [41], using the redox potential values for PQ-1 [42], is $10^{-9.2}$ at pH 7.0 in aqueous solution. The K_s of dismutation of semiquinones of tetramethyl-*p*-benzoquinone has been estimated to be 10^{-12} at pH 7.0 in aqueous solution [45]. Thus, K_s of $PQH^{\bullet}$-9 is most probably within $10^{-9} - 10^{-12}$ in aqueous solution. According to the redox properties of $PQ^{\bullet-}$-9 in aqueous solutions, the second order rate constant of Reaction 4 would be around 2×10^{8} M^{-1} s^{-1} [46]. However, as shown in Fig. 1 (B, C, E and F), both the rate of PQH_2-9 oxidation and the second order rate constant are very low, and there was no difference in oxidation of PQH_2-9 in the presence of buffers with different pH. Most probably, the very low formation of $PQH^{\bullet}$-9 in Reaction 2 is the main reason for the low rate PQH_2-9 autoxidation.

The autoxidation of PQH_2-9 in the presence of PQ-9 is also very low in organic solvents like methanol and hexane Fig. 1 (A, D). The redox potential of PQ-9/$PQ^{\bullet-}$-9 and $PQ^{\bullet-}$-9/PQ^{2-}-9 are highly negative, around -400 mV and -1100 mV vs SHE in organic solvents like dimethylforamide and acetonitrile [47, 48]. In aprotic medium, $PQ^{\bullet-}$-9 is rather stable. According to redox potential of PQ-9/$PQ^{\bullet-}$-9 and $PQ^{\bullet-}$-9/PQ^{2-}-9, the equilibrium constant K_s can be calculated as $10^{12.3}$. However, oxidation of $PQ^{\bullet-}$-9 by O_2 is unfavorable because the redox potential of $O_2/O_2^{\bullet-}$ is around -640 mV in organic solvents [49 - 51]. Protonation of $PQ^{\bullet-}$-9 and PQ^{2-}-9 lead to positive shift and decrease the difference in redox potential of PQ-9/$PQ^{\bullet-}$-9 and $PQ^{\bullet-}$-9/PQ^{2-}-9 [52]. Thus, protonation of both $PQ^{\bullet-}$-9 and PQ^{2-}-9 decreases the stability of $PQ^{\bullet-}$-9 and its redox potential becomes more positive. pK values of trimethyl-p-quinone were estimated around 20.4 and 25.5 for pK_1 and pK_2 respectively [53] and PQH_2-9 is mostly in its protonated form in organic solvents. In aprotic organic solvent, the redox potential of $O_2/O_2^{\bullet-}$ is also shifted to positive, and in the presence of a

proton donor (phenol in pyridine), the redox potential of $O_2/O_2^{\bullet-}$ is around -500 mV vs SHE [51]. The pK value for $O_2^{\bullet-}$ is 24 [49] which is higher than the pK_1 of PQH_2-9. PQH_2-9 can act as a weak proton donor for $O_2^{\bullet-}$ like phenol. According to behavior of both the quinone/hydroquinone and oxygen/superoxide systems in organic solvents [51, 52], a more negative redox potential of $O_2/HO_2^{\bullet}$, in comparison with the redox potentials of PQ-9/$PQH^{\bullet}$-9 and $PQH^{\bullet}$-9 /PQH_2-9, cause the low oxidation rate of PQH_2-9. Furthermore, the results indicate that PQH_2-9 can be rapidly oxidized by O_2 in physiological conditions only in the presence of an enzyme or a deprotonation agent. No other PQ-derivatives were detected in the autoxidation assays.

According to redox properties of PQH_2-9, the rate of autoxidation of PQH_2-9 depends on pH. The effect of a high pH was tested by addition of 1 mM KOH to solution of PQH_2-9 in methanol. In this experiment, full oxidation of PQH_2-9 was observed within 1 min (Fig. 2) with a half-time of approximately 4 s. PQH_2-9 was oxidized with biphasic kinetics that can be explained by Reactions 5-8.

$$PQH_2\text{-}9 + OH^- \rightarrow PQH^-\text{-}9 + H_2O \quad (5)$$

$$PQH^-\text{-}9 + OH^- \rightarrow PQ^{2-}\text{-}9 + H_2O \quad (6)$$

$$PQH^-\text{-}9 + O_2 \rightarrow PQ^{\bullet-}\text{-}9 + HO_2^{\bullet} \quad (7)$$

$$PQ^{2-}\text{-}9 + O_2 \rightarrow PQ^{\bullet-}\text{-}9 + O_2^{\bullet-} \quad (8)$$

$PQ^{\bullet-}$-9 is finally oxidized by O_2 to PQ-9 and $O_2^{\bullet-}$, Reaction 4

According to Reactions 4-8, deprotonation of PQH_2-9 to PQH^--9 and PQ^{2-}-9 causes rapid oxidation of PQH_2-9. The oxidation of PQ^{2-}-9 by oxygen is favorable because the redox potential of $PQ^{\bullet-}$-9/PQ^{2-}-9 is highly negative, E = -1100 mV vs SHE in organic solvents [47]. The pK_1 and pK_2 values for PQH_2-9 are (10.8 and 12.9) for aqueous solutions [43] and (20.4 and 25.5) for organic solvents [53]. Efficient autoxidation of PQH_2-9 occurs only at high pH.

The products of autoxidation of PQH_2-9 in the presence of KOH were analysed with HPLC. Typical chromatograms are shown in Fig. S1 (see Supplementary Data). As shown in Fig. 3A, the main product of autoxidation of PQH_2-9 in the presence of KOH was PQ-9. Two minor products were detected as peaks with retention times 21.8 and 40.8 min (Fig. 3C). A peak with the retention time of 21.8 min was also found to be the main product upon addition of KOH to PQ-9 solution (Figs. 3B and 3D). PQ-9-derived products are likely formed in a reaction of $O_2^{\bullet-}$ with PQ-9. $O_2^{\bullet-}$ is a product of autoxidation of PQH_2-9 (Reaction 8) but may also be generated via interaction of OH^- with PQ-9 [54].

3.2. Oxidation of PQH_2-9 by $O_2^{\bullet-}$

It is of interest to study the interaction of $O_2^{\bullet-}$ with PQH_2-9, as $O_2^{\bullet-}$ occurs as an intermediate in Reactions 5-8 and may be produced by several other mechanisms in the thylakoid membrane. $O_2^{\bullet-}$ reacts with hydroquinones in aprotic media [49], and it has been suggested that PQH_2-9 can scavenge $O_2^{\bullet-}$ inside the thylakoid membrane, forming H_2O_2 and $PQ^{\bullet-}$-9 (Reaction 9) [16, 17, 28].

$$PQH_2\text{-}9 + O_2^{\bullet-} \rightarrow PQ^{\bullet-}\text{-}9 + H_2O_2 \qquad (9)$$

The oxidation of the hydroquinone catechol to the corresponding semiquinone was shown in tetrahydrofurane upon addition of KO_2, a source of $O_2^{\bullet-}$, in the presence of crown ether that complexes K^+ from the solution [55]. To study the importance of Reaction 9, its rate was measured by following the disappearance of PQH_2-9 in acetonitrile upon addition of KO_2 in dimethylsulfoxide in the presence of crown ether using the stopped-flow method. Acetonitrile was chosen as a solvent to prevent protonation of $O_2^{\bullet-}$. The kinetics of PQH_2-9 oxidation upon addition of different concentrations of KO_2 are shown in Fig. 4.

Assuming that PQH_2-9 oxidation occurs through the irreversible Reaction 9 which is a typical second order reaction, PQH_2-9 oxidation would follow the equation

$$\frac{d[PQH_2]}{dt} = k([PQH_2]_0 - [PQH_2])([O_2^{\cdot-}]_0 - [PQH_2])$$

where $[PQH_2\text{-}9]_0$ and $[O_2^{\bullet-}]_0$ are the initial concentrations of PQH_2-9 and $O_2^{\bullet-}$,respectively, and $[PQH_2\text{-}9]$ is the variable concentration of PQH_2-9 during the reaction. The second-order rate constant was calculated from the half-time of the oxidation of PQH_2-9 according to the equation

$$k = \frac{1}{\tau_{1/2} \times ([O_2^{\cdot-}]_0 - [PQH_2]_0)} \times ln\frac{(2[O_2^{\cdot-}]_0 - [PQH_2]_0)}{[O_2^{\cdot-}]_0}$$

However, it was found that the rate constant increased with $O_2^{\bullet-}$ concentration (Fig. 5) and the kinetic curve of PQH_2-9 oxidation by 500 µM or 1 M KO_2 obviously deviated from second order (Fig. 4). At higher concentrations of $O_2^{\bullet-}$, oxidation of PQH_2-9 more closely resembled a typical second-order reaction. The complicated kinetic pattern indicates that oxidation of PQH_2-9 by $O_2^{\bullet-}$ is realized via deprotonation or hydrogen abstraction mechanisms that involve several reactions. In the following, the reaction series will be worked out.

According to its thermodynamic properties, $O_2^{\bullet-}$ can act as a strong reductant in an aprotic medium because the midpoint potential (Em) of $O_2/O_2^{\bullet-}$ is around -640 mV in an

aprotic organic solvent like acetonitrile [49 - 51]. At a very negative potential, $O_2^{\bullet-}$ can be reduced to a highly unstable peroxide ion; the redox potential of $O_2^{\bullet-}/O_2^{2-}$ is -2V [56]. In an aprotic medium, $O_2^{\bullet-}$ is a strong deprotonation agent with pK of approximately 24 [49]. Therefore $O_2^{\bullet-}$ is able to oxidize lipophilic compounds in aprotic media via a deprotonation mechanism [57]. $O_2^{\bullet-}$ is a powerful nucleophile and can be involved in nucleophilic reactions with various organic compounds [49].

Two mechanisms have been suggested for oxidation of hydroquinones by $O_2^{\bullet-}$ in aprotic media [49, 57]. These mechanisms can be realized for oxidation of PQH_2-9 as follows. (i) A one-step mechanism where $O_2^{\bullet-}$ interacts with a hydroquinone to form an intermediate complex that can decompose to $PQ^{\bullet-}$-9 and H_2O_2, Reaction 10:

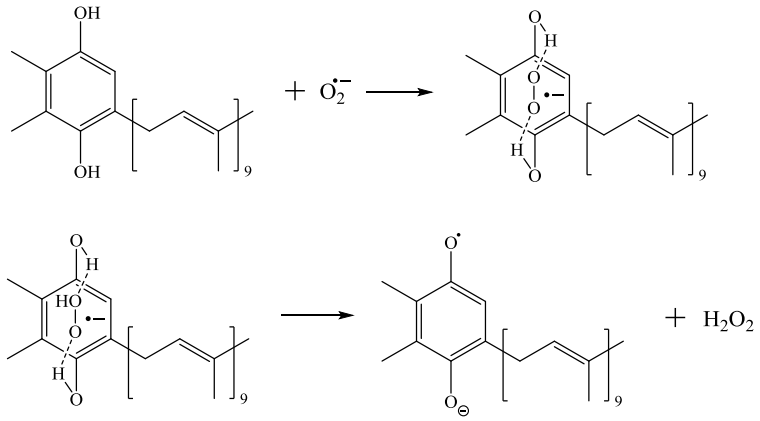

(10)

(ii) Alternatively, a two-step mechanism with hydrogen abstraction (Reaction 11)

$$PQH_2\text{-}9 + O_2^{\bullet-} \rightarrow PQH^{\bullet}\text{-}9 + HO_2^{-} \quad (11)$$

or deprotonation (Reaction 12)

$$PQH_2\text{-}9 + O_2^{\bullet-} \leftrightarrows PQH^{-}\text{-}9 + HO_2^{\bullet} \quad (12)$$

can start PQH_2-9 oxidation.

After the initiation of the two-step mechanism, PQH_2-9 oxidation may proceed through Reactions 13-14:

$$PQH^{-}\text{-}9 + HO_2^{\bullet} \rightarrow PQH^{\bullet}\text{-}9 + HO_2^{-} \quad (13)$$

$$PQH^{\bullet}\text{-}9 + HO_2^{-} \leftrightarrows PQ^{\bullet-}\text{-}9 + H_2O_2 \quad (14)$$

Finally, $PQ^{\bullet-}$-9 can be oxidized by O_2 with formation of $O_2^{\bullet-}$ and PQ-9 (Reaction 4).

Oxidation of PQH_2-9 via the hydrogen abstraction (Reaction 11) or the deprotonation mechanism (Reactions 12 and 13) leads to formation of $PQH^{\bullet}$-9 which can react with another molecule of $PQH^{\bullet}$-9 to form PQH_2-9 (Reaction 2). Thus, the actual rate of PQH_2-9 oxidation would differ from the apparent rate because PQH_2-9 is produced by Reaction 2. Obviously, Reaction 2 explains why the kinetics of PQH_2-9 oxidation differ from the kinetic curve of a second order reaction (Fig. 4). Oxidation of PQH_2-9 by $O_2^{\bullet-}$ would actually be even more complicated than Reactions 11-14 suggest, as $HO_2^{\bullet}$ can react with $PQH^{\bullet}$-9 (Reaction 15) and thereby suppress Reaction 2.

$$PQH^{\bullet}\text{-}9 + HO_2^{\bullet} \rightarrow PQ\text{-}9 + H_2O_2 \qquad (15)$$

Furthermore, $HO_2^{\bullet}$ can react with PQH_2-9 to form $PQH^{\bullet}$-9 and H_2O_2 (Reaction 16).

$$PQH_2\text{-}9 + HO_2^{\bullet} \rightarrow PQH^{\bullet}\text{-}9 + H_2O_2 \qquad (16)$$

Oxidation of PQH_2-9 by $HO_2^{\bullet}$ increases the apparent rate of PQH_2-9 oxidation. On the other hand, Reaction 16 produces $PQH^{\bullet}$-9 that can be involved in Reaction 2 which produces PQH_2-9. $HO_2^{\bullet}$ can also be scavenged via disproportionation (Reaction 17)

$$HO_2^{\bullet} + HO_2^{\bullet} \rightarrow H_2O_2 + O_2 \qquad (17)$$

or either by $O_2^{\bullet-}$ or by $PQ^{\bullet-}$-9 (Reactions 18 and 19):

$$HO_2^{\bullet} + O_2^{\bullet-} \rightarrow HO_2^{-} + O_2 \qquad (18)$$

$$PQ^{\bullet-}\text{-}9 + HO_2^{\bullet} \rightarrow PQ\text{-}9 + HO_2^{-} \qquad (19)$$

Scavenging of $HO_2^{\bullet}$ would eliminate the influence of $HO_2^{\bullet}$ on the apparent rate of PQH_2-9 oxidation. However, it is difficult to estimate the efficiency of $HO_2^{\bullet}$ scavenging.

$O_2^{\bullet-}$ is able to react with $PQH^{\bullet}$-9 to form PQ-9 and HO_2^{-} (Reaction 20).

$$PQH^{\bullet}\text{-}9 + O_2^{\bullet-} \rightarrow PQ\text{-}9 + HO_2^{-} \qquad (20)$$

Reaction 20 prevents the dismutation of $PQH^{\bullet}$-9. Thus, the rate of PQH_2-9 oxidation by $O_2^{\bullet-}$, measured as a decrease fluorescence intensity at 330 nm, reflects the total rate of PQH_2-9 oxidation due to Reactions 2 and 11-20. The apparent rate of PQH_2-9 oxidation will trend to the actual rate of PQH_2-9 oxidation with increasing concentration of $O_2^{\bullet-}$, and thereby the rate constant should be calculated from an asymptotic fit when concentration of $O_2^{\bullet-}$

approaches infinity (Fig. 5). With this method, the rate constant was estimated to be 4.06 × 10^4 M^{-1} s^{-1}.

According to the above two-step mechanism, the oxidation of PQH_2-9 by $O_2^{\bullet-}$ in an aprotic medium leads to formation of PQ-9, a stable compound. However, exposure of PQH_2-9 to KO_2 caused the formation of PQ-9, but PQ-9 first increased with increasing KO_2 concentration and disappeared with a higher concentration (Fig. 6A), and exposure of PQ-9 to KO_2 led to disappearance of PQ-9 with increasing KO_2 concentration (Fig. 6B). Seven PQ-derivatives were detected under exposure of PQH_2-9 to KO_2 (Fig. 6C). The same PQ-derivatives, excluding the PQ-derivative with retention time 12.1 min, were formed under exposure of PQ-9 to KO_2 in acetonitrile (Fig. 6D). See Fig. S2 for typical chromatograms and Fig. S3 for the absorption spectra of the PQ-derivatives.

Most probably, the PQ-derivatives (Figs. 6C and D) are produced in reactions of $O_2^{\bullet-}$ with PQ-9 formed by oxidation of PQH_2-9. PQ-derivatives with retention times of 12.1, 14.3, 20.4, 21.8 and 40.8 min were formed at $O_2^{\bullet-}$concentrations from 0 to 0.5 mM. At higher $O_2^{\bullet-}$ concentrations, these initial PQ-derivatives were transformed to compounds with retention times 17.1, 22.8 and 25.6 min. (Figs. 6C and D). Thus, both formation of the initial PQ-derivatives and their transformation seem to depend on $O_2^{\bullet-}$. The structures of the PQ-derivatives were not determined in this work. Most probably, the PQ-derivatives are formed via nucleophilic reactions of $O_2^{\bullet-}$ with both the quinone ring and the isoprene side chain of PQ-9.

It seems that the formation of PQ-derivatives is proton independent, as the PQ-derivatives were formed by a reaction of $O_2^{\bullet-}$ with PQ-9 in the absence of proton donors. The observation of the PQ-derivatives in these experiments also suggests that $O_2^{\bullet-}$, according to its general properties [49], is a strong nucleophilic agent against PQ. According to our analysis, the hydroperoxyl radical $HO_2^{\bullet}$ would rather take part in deprotonation pathways or reactions with the semiquinones (Reactions 13-20).

3.3. Oxidation of PQH_2-9 by H_2O_2

The reduction of oxygen in the PQ-pool leads to formation of H_2O_2 [17]. H_2O_2 can be formed via oxidation of PQH_2-9 by $O_2^{\bullet-}$ via Reactions 11-14, and we have recently shown that H_2O_2 can also be produced in a reaction between PQH_2-9 and $^1O_2$ [34]. Both mechanisms of H_2O_2 formation function within the thylakoid membrane [17, 34]. H_2O_2 that exits the membrane can be scavenged in MPR. However, there is no earlier data about scavenging of H_2O_2 inside the thylakoid membrane. To check the effect of H_2O_2 on both PQ-9 and PQH_2-9,

aqueous H_2O_2 was added to samples containing PQ-9, PQH_2-9 or a mixture of PQH_2-9 and PQ-9 in methanol. As shown in Fig. S4, H_2O_2 oxidized PQH_2-9 to PQ-9 (A, B) but did not react with PQ-9 (C, D). No additional peaks were observed, indicating that no PQ-derivatives were produced. The oxidation of PQH_2-9 observed 2 min after addition of H_2O_2 increased with the concentration of H_2O_2 (Fig. 7A) but prolonging the incubation time to 40 min only caused a minor additional increase in the conversion of PQH_2-9 to PQ-9 (Fig. 7B). Thus, the oxidation of PQH_2-9 by H_2O_2 mainly occurred in 2 min or less. Only a fraction of PQH_2-9 was oxidized by H_2O_2 although the concentration of H_2O_2 was much higher than that of PQH_2-9. For example, only 25% of 75 µM PQH_2-9 was oxidized by 5 mM H_2O_2 (Fig. 7A). The reaction caused only a minor decrease in the concentration of H_2O_2, as after 2 min of reaction with the initial H_2O_2 concentration of 5 mM, the concentration of H_2O_2 was still higher than 4 mM (data not shown).

We suggest that the oxidation of PQH_2-9 by H_2O_2 proceeds via a deprotonation mechanism that produces PQH^--9, PQ^{2-}-9 and protonated hydrogen peroxide cation ($H_3O_2^+$), Reactions 22 and 23.

$$PQH_2\text{-}9 + H_2O_2 \leftrightarrows PQH^-\text{-}9 + H_3O_2^+ \quad (22)$$

$$PQH^-\text{-}9 + H_2O_2 \leftrightarrows PQ^{2-}\text{-}9 + H_3O_2^+ \quad (23)$$

PQH^--9 and PQ^{2-}-9 are subsequently oxidized by O_2 via Reactions 7, 8 and 4, with PQ-9, $HO_2^\bullet$ and $O_2^{\bullet-}$ as end products.

$H_3O_2^+$ is known to be formed in an acidic hydrogen peroxide solution [58, 59]. Both PQH_2-9 and PQH^--9 can function as proton donors, and therefore deprotonation of PQH_2-9 and PQH^--9 by H_2O_2 via Reactions 22 and 23 can occur. Accumulation of $H_3O_2^+$ may prevent further deprotonation of PQH_2-9 due to the reversibility of Reactions 22 and 23.

4. Discussion

4.1. Oxidation of PQH_2-9 to PQ-9 by O_2, O_2^- and $^1O_2$

In addition to its role in linear electron flow, PQH_2-9 is oxidized by an autoxidation reaction, oxygen-dependent reactions with Cyt b_{559} and with Cyt b_6/f, PTOX-catalyzed reactions and via oxidation by $^1O_2$. These pathways will be collectively called as oxygen-dependent oxidation of PQH_2-9, as oxygen acts as the ultimate oxidant in all of them. Most

pathways produce PQ-9 as the main product of oxidation. We will first describe the reaction mechanisms and then discuss their rates.

Autoxidation. Autoxidation of PQH_2-9 by O_2 can occur both inside and on the surface of the thylakoid membrane [17], and within PSII via the quinone binding sites Q_C and Q_D [60]. The autoxidation starts by production of $PQH^{\bullet}$-9 (Reaction 2), deprotonation of $PQH^{\bullet}$-9 (Reaction 3) and subsequent oxidation of $PQ^{\bullet-}$-9 by O_2 with the formation of $O_2^{\bullet-}$ and PQ-9 (Reaction 4). Furthermore, PQH_2-9 can be oxidized by $O_2^{\bullet-}$ (Reaction 9). This reaction produces $PQ^{\bullet-}$-9 that would again react with O_2 to produce $O_2^{\bullet-}$ and PQ-9.

Reactions catalyzed by Cyt *b*$_{559}$. The low-potential form of Cyt *b*$_{559}$ (Cyt *b*$_{559}$LP) can transfer electrons to oxygen [26, 61] and act as a PQH_2:O_2 oxidoreductase if the PQ-pool is highly reduced. Reduction of Cyt *b*$_{559}$ by PQH_2-9 occurs via the specific quinol/guinone-binding sites Q_C and Q_D in Photosystem II [60, 62]. Cyt *b*$_{559}$ may actually mediate a series of reactions (Fig. 8). In the first phase, interaction of PQH_2-9 with oxidized Cyt *b*$_{559}$ initiates a reaction series that produces $O_2^{\bullet-}$ (Fig. 8A) and in the second phase, $O_2^{\bullet-}$ forms H_2O_2 by oxidizing both reduced Cyt *b*$_{559}$ and PQH_2-9 (Fig. 8B). In Reaction I, reduction of Cyt *b*$_{559}$ by PQH_2-9 causes formation of a Cyt $b_{559}^{red}(H^+)PQH^{\bullet}$-9 complex [62] that can decompose to form $PQH^{\bullet}$-9 (Reactions II and III). Cyt b_{559}^{red} can react with PQ-9 forming $PQ^{\bullet-}$ [61] (Reaction VII). Reaction of $PQH^{\bullet}$-9 with O_2 produces $HO_2^{\bullet}$ and reaction of $PQ^{\bullet-}$-9 with O_2 produces $O_2^{\bullet-}$ (Reactions IV and VI, respectively). Reaction VI is faster than Reaction IV because the redox potential of $PQH^{\bullet}$ depends on pH [42], and therefore deprotonation of $PQH^{\bullet}$-9 to $PQ^{\bullet-}$-9 (Reaction V) may occur before formation of $O_2^{\bullet-}$. Direct reduction of O_2 by Cyt *b*$_{559}$ produces $O_2^{\bullet-}$ (Reaction VIII).

In the second phase of the reaction series catalyzed by Cyt *b*$_{559}$, $O_2^{\bullet-}$ and $HO_2^{\bullet}$ can oxidize PQH_2-9 to $PQH^{\bullet}$-9/$PQ^{\bullet-}$-9 (Reactions IX and X, respectively). This reaction can proceed in aprotic medium because the second order rate constant of this reaction is around 4.06×10^4 M^{-1} s^{-1}. In addition, $O_2^{\bullet-}$ and $HO_2^{\bullet}$ can react with Cyt b_{559}^{red} (Reactions XI and XII, respectively) [9]. In both cases, H_2O_2 would be formed within the thylakoid membrane. Thus, $O_2^{\bullet-}$ accelerates oxidation of PQH_2-9 in Cyt *b*$_{559}$. The oxidation of PQH_2-9 leads to the formation of $PQH^{\bullet}$-9/$PQ^{\bullet-}$-9, which may further reduce O_2 to $O_2^{\bullet-}$. The final products of the reactions between PQH_2-9 and O_2, catalyzed by Cyt *b*$_{559}$, are PQ-9, $O_2^{\bullet-}$ and H_2O_2.

Reactions catalyzed by Cyt *b*$_6$*f* with oxygen as electron acceptor. In addition to the function of Cyt *b*$_6$*f* in linear electron flow, Cyt *b*$_6$*f* can oxidize PQH_2-9 in a reaction that produces $O_2^{\bullet-}$ and H_2O_2 [18]. The oxygen-dependent reactions begin with oxidation of PQH_2-

9 at the quinone oxidation site of Cyt b_6/f (Reactions 24 and 25); an iron-sulfur center FeS and a low-potential heme of Cyt *b* (Cyt bL) act as electron acceptors.

$$PQH_2\text{-}9 + FeS_{ox} \rightarrow PQH^{\bullet}\text{-}9 + FeS_{red} + H^+ \quad (24)$$

$$PQH^{\bullet}\text{-}9 + \text{Cyt } bL_{ox} \rightarrow PQ\text{-}9 + \text{Cyt } bL_{red} + H^+ \quad (25)$$

$O_2^{\bullet-}$ and H_2O_2 can be generated by Cyt bL by Reactions 26 and 27.

$$\text{Cyt } bL_{red} + O_2 \rightarrow O_2^{\bullet-} + \text{Cyt } bL_{ox} \quad (26)$$

$$\text{Cyt } bL_{red} + O_2^{\bullet-} + 2H^+ \rightarrow + \text{Cyt } bL_{ox} + H_2O_2 \quad (27)$$

Furthermore, $PQH^{\bullet}$-9 that occurs as an intermediate of oxidation of PQH_2-9 [18] in Reactions 24-25 can produce $O_2^{\bullet-}$ and H_2O_2 via Reactions 3, 4, 9 and 17. The formation of $O_2^{\bullet-}$ via the Cyt b_6/f pathway would probably depend on pH because of the pH dependence of the redox potential of $PQH^{\bullet}$-9.

Oxidation of PQH_2-9 by PTOX. PTOX reduces O_2 using PQH_2-9 as an electron donor via Reaction 28 without formation of ROS.

$$2PQH_2\text{-}9 + O_2 \rightarrow 2PQ\text{-}9 + 2H_2O \quad (28)$$

However, isolated PTOX can oxidize decylPQH2 with formation of ($O_2^{\bullet-}$ or H_2O_2) at pH 8.0 or substrate limiting concentrations [21]. In this case, $O_2^{\bullet-}$can be generated either through formation of $PQH^{\bullet}$-9 which can be deprotonated and then oxidized by O_2 or by the reduction of oxygen at the catalytic non-heme diiron center of PTOX [21].

Oxidation of PQH_2-9 by $^1O_2$. Finally, PQH_2-9 can be oxidized by $^1O_2$ that reacts with PQH_2-9, producing PQ-9 and H_2O_2 as the main products [30-34]. The second order rate constant of the reaction of $^1O_2$ with PQH_2-9 is $0.97 \pm 0.08 \times 10^8$ M^{-1} s^{-1} [12]. Because $^1O_2$ mainly originates in the reaction center of PSII in the light, $^1O_2$ dependent oxidation of PQH_2-9 would require light for production of both substrates PQH_2-9 and $^1O_2$.

4.2. Rates of ROS-dependent oxidation of PQH_2-9 in thylakoid membranes

Oxygen-dependent oxidation of PQH_2-9. All mechanisms of oxidation of PQH_2-9 other than linear electron flow will be referred to as oxygen-dependent mechanisms because all have oxygen as the final electron acceptor. The rates of the reactions will be considered separately for light and darkness. Furthermore, the rates of oxidation of PQH_2-9, and the associated production of ROS, will be discussed separately for the hydrophobic core of the membrane and for the membrane surface. The latter discussion is considered necessary even for reactions catalyzed by protein complexes with known locations because oxygen concentration has a gradient rather than makes an abrupt 10 fold change when going from the soluble phase to the membrane.

Rate of oxidation of PQH_2-9 in the dark. The rate of PQH_2-9 oxidation after photoreduction in the dark was measured earlier by monitoring absorbance changes associated with the conversion of PQH_2-9 to PQ-9 in isolated thylakoids and can be calculated to be 0.9 μmol PQH_2-9 $(mg\ Chl)^{-1}\ h^{-1}$ [26]. The rate of PQH_2-9 oxidation was calculated from second order rate constants with the following conditions: volume of chloroplast, 3.6×10^{-5} L $(mg\ Chl)^{-1}$ [63]; volume of thylakoid membrane, 4.6×10^{-6} L $(mg\ Chl)^{-1}$ [63]; molar mass of chlorophyll, 894 g mol^{-1} [63]; amount of photoactive PQH_2-9 in thylakoids, 14×10^{-3} mol $(mol\ Chl)^{-1}$ [26]; concentration of oxygen inside the membrane and on the membrane surface, 2.4 mM and 253 μM, respectively [26]. On the basis of the above experimental data [26], the second order rate constants of PQH_2-9 oxidation in thylakoids after photoreduction were estimated to be 6.3 $M^{-1}\ s^{-1}$ and 63 $M^{-1}\ s^{-1}$ for oxygen concentrations 2.4 mM and 253 μM, respectively [26]. With these rate constants, the rates of dark oxidation of PQH_2-9 inside and on the surface of the thylakoid membrane would be 5.14×10^{-5} and 7.94×10^{-6} M s^{-1}, respectively (Table 2). The rates and second order rate constants for oxidation were calculated assuming even distribution of PQH_2-9 in the volume of the stroma (for calculations concerning the membrane surface) and volume of thylakoid membrane (for calculations concerning reactions inside the membrane).

Rate of autoxidation. The second order rate constant of autoxidation of PQH_2-9 in the presence of PQ-9 (added to provide the other precursor for the dismutation, Reaction 2) in organic solvents like methanol and hexane was small and independent of pH of buffers added to organic solvents. With the above assumptions, the rates of PQH_2-9 autoxidation via dismutation inside and on the surface of the thylakoid membrane would be 1.05×10^{-8} and 2.3×10^{-9} M s^{-1}, respectively (Table 2).

Autoxidation does not explain O_2 consumption in the light in presence of an inhibitor of Cyt *b_6f*. The rate of PQH_2-9 oxidation in thylakoids in the light can be calculated from the oxygen consumption rate when oxidation of PQH_2-9 by Cyt *b_6f* is

inhibited. In this way, the maximum rate of oxygen consumption associated with PQH_2-9 oxidation was measured to be approximately 10 µmol O_2 (mg Chl)$^{-1}$ h^{-1}, or 20 µmol PQH_2-9 (mg Chl)$^{-1}$ h^{-1} [17]. This rate is over 20 times as fast as the rate of oxidation of PQH_2-9 in the dark after photoreduction [26], suggesting that light-dependent reaction(s) dominate the oxygen-dependent oxidation of PQH_2-9. With these data, the rates of oxidation of PQH_2-9 inside and on the surface of the thylakoid membrane would be 1.21×10^{-3} M s^{-1} and 1.8×10^{-4} M s^{-1}, respectively (Table 2), and the respective second order rate constants of PQH_2-9 oxidation would be 1.48×10^{2} and 1.43×10^{3} M^{-1} s^{-1} for reactions inside and on the surface of the thylakoid membrane, respectively. Thus, the rates of PQH_2-9 oxidation inside and on the surface of the thylakoid membrane in the light are 10^5 times as high as the rate of autoxidation of pure PQH_2-9 in organic solvents (Table 2). The dark rates of oxidation of PQH_2-9 in and on the thylakoid membrane, 5.14×10^{-5} and 7.94×10^{-6} Ms^{-1}, respectively, are 10^3 times as high as the respective rates of dismutation-dependent autoxidation of PQH_2-9 in organic solvents (Table 2). These data indicate that dismutation (Reaction 2) cannot be responsible for oxygen-dependent oxidation of PQH_2-9 in thylakoids.

Rate of Cyt *b*$_{559}$ dependent oxidation of PHQ_2-9. The rate of Cyt *b*$_{559}$LP oxidation by O_2 [26] in and on the surface of the thylakoid membrane would be 9.64×10^{-7} M s^{-1} and 1.47×10^{-7} M s^{-1} assuming even distribution of Cyt *b*$_{559}$ in the volume of the thylakoid membrane (for calculations in the membrane) and in the volume of the stroma (for calculations concerning the membrane surface) ([26]; Table 2). These rates are roughly 50 times slower than the rate of PQH_2-9 oxidation in thylakoids in the dark and 10^3 fold slower than the oxygen-dependent oxidation of PQH_2-9 in thylakoid membranes in the light (Table 2). Thus, direct oxidation of reduced Cyt *b*$_{559}$LP by O_2 cannot provide the observed rates of PQH_2-9 oxidation in thylakoid membranes in the dark.

Role of Cyt b$_6$/f in oxygen consumption in thylakoid membranes. The rate of $O_2^{\bullet-}$ generation by Cyt *b*$_6$*f* was estimated to be 2.6×10^{-3} mol (mol Chl)$^{-1}$ s-^{1} [18] which would suggest that the rate of Cyt *b*$_6$*f* oxidation by O_2 is 6.3×10^{-4} M s^{-1} or 9.2×10^{-5} M s^{-1} for reactions in and on the membrane surface, respectively. Assuming that the ratio of Cyt *b*$_6$*f* to PSI is 1:1 and the ratio of Cyt *b*$_6$*f* to Chl is 1:420 [64], the second order rate constants of oxidation of PQH_2-9 in and on the membrane are 5.07×10^{2} M^{-1} s^{-1} and 4.29×10^{3} M^{-1} s^{-1}, respectively (Table 2). The second order rate constants were calculated assuming an even distribution of Cyt *b*$_6$*f* in the volume of the thylakoid membrane (for membrane) and the volume of the stroma (for membrane surface). Based on these data, the rate of Cyt *b*$_6$*f*-catalyzed oxidation of PQH_2-9 by O_2 would account for approximately half of the rate of PQH_2-9 oxidation in thylakoids in the light (Table 2). However, the formation of $O_2^{\bullet-}$ by Cyt

b_6/f was inhibited by DBMIB which prevents the oxidation of PQH_2-9 by the Rieske iron-sulfur protein [18]. Therefore, oxygen consumption in the presence of DNP-INT, another inhibitor of PQH_2-9 oxidation by the Rieske protein [17] cannot be associated with the Cyt *b_6/f* pathway, indicating that reduction of O_2 by Cyt bL does not explain oxygen-dependent oxidation of PQH_2-9.

Role of PTOX in oxygen consumption in thylakoid membranes. The rate of PTOX mediated electron flow is approximately 0.3 e^- s^{-1} $PSII^{-1}$ [22]. This gives the rate of PQH_2-9 oxidation equal to 0.15 PQH_2-9 $PSII^{-1}$ s^{-1}, or 0.35 μmol PQH_2-9 (0.7 μmol O_2) $(mg\ Chl)^{-1}$ h^{-1}, assuming that the ratio of PSII to Chl is 1:420 [64]. Thus, the rate of PQH_2-9 oxidation can be estimated to be 8.68×10^{-5} M s^{-1} or 1.27×10^{-5} M s^{-1} for reactions in and on the membrane surface, respectively (Table 2). These rates are similar to the overall rates of oxidation of PQH_2-9 in thylakoid membranes in the dark (Table 2). The second order rate constants of PTOX-mediated oxidation of PQH_2-9 in and on the membrane are 10.6 M^{-1} s^{-1} and 1.01×10^2 M^{-1} s^{-1}, respectively (Table 2).

In the light, oxidation of PQH_2-9 by PTOX would not lead to consumption because of matching stoichiometry with oxygen production by PSII, Reactions 28 and 29.

$$2PQH_2\text{-}9 + O_2 \rightarrow 2PQ\text{-}9 + 2H_2O \quad (28)$$

$$PS\ II + 2H_2O + 2PQ\text{-}9 \rightarrow 2PQH_2\text{-}9 + O_2 \quad (29)$$

Reaction 28 does not lead to formation of ROS. However, isolated PTOX can oxidize decylPQH_2 with formation of ($O_2^{\bullet-}$ or H_2O_2) at pH 8.0 or substrate limiting concentrations [21]. In this case, the efficiency of ROS production by PTOX was estimated to be around 17 % of the total oxygen reducing activity of PTOX. Thus, the rate of PTOX-mediated PQH_2-9 oxidation associated with formation of H_2O_2 can reach 1.47×10^{-5} M s^{-1} or 2.16×10^{-6} M s^{-1} for reactions in and on the membrane surface, respectively (Table 2). The second order rate constants of oxidation of PQH_2-9 associated with formation of $O_2^{\bullet-}$ or H_2O_2 can be estimated to be 1.8 M^{-1} s^{-1} and 17 M^{-1} s^{-1} inside and on the membrane, respectively (Table 2). The rate of PTOX-mediated PQH_2-9 oxidation is approximately one fourth of the rate of oxygen-dependent oxidation of PQH_2-9 in the dark.

As shown in Table 2, the rate of PQH_2-9 oxidation by a PTOX-mediated reaction [22] is close to the rate of dark oxidation of PQH_2-9 after photoreduction [26]. Taking into account that Cyt *b_{559}* dependent oxidation is slower than the dark oxidation of PQH_2-9, the dark oxidation of PQH_2-9 can mostly be assigned to the PTOX reaction. Nevertheless, the *Cyt b_{559}* mediated oxidation of PQH_2-9 according to reactions (Fig. 8) can also take place.

Oxygen consumption in the light suggest a role for $^1O_2$. Oxygen-dependent oxidation of PQH_2-9 increases by over 20 fold by illumination (Table 2). Additional

oxidation of PQH_2-9 in the light can be partially mediated by $^1O_2$ generated by PSII in the light, as $^1O_2$ oxidizes PQH_2-9 to PQ-9 with a high second order rate constant, around 10^8 M^{-1} s^{-1} [12]. H_2O_2 is formed as a byproduct of this reaction [34]. However, oxygen consumption in the presence of DNP-INT was saturated at the low photosynthetic photon flux density of 30-60 µmol $m^{-2}s^{-1}$ [17], suggesting that in addition to formation of $^1O_2$, other mechanisms contribute to oxygen consumption.

In conclusion, we suggest that the oxygen-dependent oxidation of PQH_2-9 proceeds simultaneously via five independent mechanisms (Fig. 9): (a) Cyt b_{559} mediated oxidation of PQH_2-9 with formation of $O_2^{\bullet-}/HO_2^{\bullet}$ within the thylakoid membrane (Fig. 8), (b) a PSII-dependent mechanism in which $^1O_2$ formed in PSII reacts with PQH_2-9, (c) formation of $O_2^{\bullet-}$ and H_2O_2 after oxidation of PQH_2-9 by Cyt b_6/f, (d) PSI-dependent mechanism in which $O_2^{\bullet-}$ formed in PSI reacts with PQH_2-9, (e) PTOX mediated oxidation of PQH_2-9, part of which leads to formation of $O_2^{\bullet-}$ and H_2O_2.

4.3. Formation of the hydroxyl radical in PSI may depend on intramembraneous H_2O_2

Generation of $O_2^{\bullet-}$ has been suggested to occur at the phylloquinone (PhQ) site (A1) [29, 65] of PSI. In the presence of PQH_2-9, production of $O_2^{\bullet-}$ would lead to formation of H_2O_2 (Fig. 9). The redox potential of $H_2O_2/(HO^{\bullet}, {}^{-}OH)$ is 400–600 mV in organic solvents [66] whereas the redox potentials of PhQ/ $PhQ^{\bullet-}$ at $A1_A$ and $A1_B$ are -671 and -844 mV, respectively [67]. Thus, the presence of H_2O_2 in the vicinity of the A1 site would lead to the formation of the highly reactive hydroxyl radical $HO^{\bullet}$ in a Fenton reaction (Reaction 30) [68]

$$PhQ^{\bullet-} + H_2O_2 \rightarrow PhQ + HO^{\bullet} + {}^{-}OH. \quad (30)$$

The production of $HO^{\bullet}$ near to the reaction center of PSI may contribute to the photoinhibition of PSI. Formation of $HO^{\bullet}$ via reaction of $O_2^{\bullet-}$ with the terminal acceptors F_X, F_A, and F_B of PSI was recently suggested [65]. However, this route of $HO^{\bullet}$ formation would require dismutation of $O_2^{\bullet-}$ to form H_2O_2 as an intermediate, and efficient scavenging of H_2O_2 in the chloroplast stroma would therefore limit $HO^{\bullet}$ formation. Intramembraneous H_2O_2, in turn, is not efficiently scavenged.

4.4. Oxygen reduction in the membrane and in the soluble phase

The rates of $O_2^{\bullet-}$ production by Mehler's reaction were estimated to be 0.9×10^{-3} M s^{-1} and 1.3×10^{-4} M s^{-1} for oxygen reduction in and on the membrane respectively, which

implies that the rate of PSI-dependent $O_2^{\bullet-}$ production is around 15 µmol $O_2^{\bullet-}$ (mg Chl)$^{-1}$ h^{-1} [14, 16]. If the ratio of PSI to Chl in chloroplasts is 1:420 [64], then the second order rate constants of oxidation of PSI by O_2 are 7.24×10^2 M^{-1} s^{-1} and 6.07×10^3 M^{-1} s^{-1} for thylakoid membrane and membrane surface respectively. Thus, the second order rate constants for reduction of O_2 by PSI are close to the second order rate constants for oxidation of PQH_2-9 by O_2 in the thylakoid membrane in the light (Table 2). In isolated thylakoids, the ratio between Mehler's reaction and PQ pool-depended O_2 reduction was measured to be 4:1 in low light and 1:3 in high light [16], indicating that intramembranous formation of ROS via the PQ pool-dependent pathway can be significant in the light.

4.5. Role of PQ/PQH_2 and robustness of the data

The present work compiles data from the experiments with data from several laboratories working on both quinones and thylakoid protein complexes. Therefore some uncertainty in the data cannot be avoided, especially when it comes to the reactions of the thylakoid protein complexes in which biological variation may also play a role.

It could be asked whether the PQ pool of thylakoids should be considered a ROS producing or a ROS scavenging unit. The present experiments do not give an answer because the reactions do not cancel each other, and some ROS scavenging reactions like the reaction between $^1O_2$ and PQH_2 also produce ROS.

Acknowledgments

The authors wish to thank Matti Turtola and Georgi Belogurov for help with rapid kinetic measurements. Funding: This study was financially supported by Academy of Finland [grant number 307335].

References

[1] C. Myake, Alternative electron flows (water-water cycle and cyclic electron flow around PSI) in photosynthesis: molecular mechanisms and physiological functions, Plant Cell Physiol. 51 (2010) 1951–1963.
[2] U. Heber, Irrungen, Wirrungen? The Mehler reaction in relation to cyclic electron transport in C3 plants, Photosynth. Res. 73 (2002) 223 – 231.
[3] G. Peltier, D. Tolleter, E. Billon, L. Cournac, Auxiliary electron transport pathways in chloroplasts of microalgae, Photosynth. Res. 106 (2010) 19 – 31.
[4] K. Asada, Production and scavenging of reactive oxygen species in chloroplasts and their functions, Plant Physiol. 141 (2006) 391–396.
[5] K.-J. Dietz, I. Turkan, A. Krieger-Liszkay, Redox- and reactive oxygen species-dependent signaling into and out of the photosynthesizing chloroplast. Plant Physiol. 171 (2016) 1541–1550.
[6] K. Apel, H. Hirt, Reactive oxygen species: Metabolism, oxidative stress, and signal transduction. Annu. Rev. Plant Biol. 5 (2004) 373–99.
[7] F. Van Breusegem, J. Bailey-Serres, R. Mittler, Unraveling the tapestry of networks involving reactive oxygen species in plants. Plant Physiol. 147 (2008) 978–984.
[8] C.H. Foyer, G. Noctor, Ascorbate and glutathione: the heart of the redox hub. Plant Physiol. 155 (2011) 2-18.
[9] P. Pospíšil, Molecular mechanisms of production and scavenging of reactive oxygen species by photosystem II, Biochim. Biophys. Acta 1817 (2012) 218–231.
[10] A. Krieger-Liszkay, C. Fufezan, A. Trebst, Singlet oxygen production in photosystem II and related protection mechanism, Photosynth. Res. 98 (2008) 551–564.
[11] E. Tyystjärvi, Photoinhibition of Photosystem II, Int. Rev. Cell Mol. Biol. 300 (2013) 243–303.
[12] J. Gruszka, A. Pawlak, J. Kruk, Tocochromanols, plastoquinol, and other biological prenyllipids as singlet oxygen quenchers – determination of singlet oxygen quenching rate constants and oxidation products. Free Radic. Biol. Med. 45 (2008) 920–928.
[13] S. Munné-Bosch, L. Alegre, The function of tocopherols and tocotrienols in plants. Crit Rev. Plant Sci. 21 (2002), 31–57.
[14] K. Asada, The water–water cycle in chloroplasts: scavenging of active oxygens and dissipation of excess photons, Annu. Rev. Plant Physiol. Plant Mol. Biol. 50 (1999) 601 – 639 .
[15] K. Asada, K. Kiso, K. Yoshikawa, Univalent reduction of molecular oxygen by spinach chloroplasts on illumination. J. Biol. Chem. 249 (1974) 2175–2181.
[16] S. Khorobrykh, M. Mubarakshina, B. Ivanov, Photosystem I is not solely responsible for oxygen reduction in isolated thylakoids. Biochim. Biophys. Acta 1657 (2004) 164–167.
[17] S.A. Khorobrykh, B.N. Ivanov, Oxygen reduction in a plastoquinone pool of isolated pea thylakoids. Photosynth. Res. 71 (2002) 209–219.
[18] D. Baniulis, S. Saif Hasan, J. T. Stofleth, W. A. Cramer, Mechanism of enhanced superoxide production in the Cytochrome b_6f complex of oxygenic photosynthesis. Biochemistry 52 (2013) 8975–8983.
[19] W.J. Nawrocki, N.J. Tourasse, A. Taly, F. Rappaport, F.A. Wollman, The plastid terminal oxidase: its elusive function points to multiple contributions to plastid physiology. Annu. Rev. Plant Biol. 66 (2015) 49−74.
[20] A. Krieger-Liszkay, K. Feilke, The dual role of the plastid terminal oxidase PTOX: between a protective and a pro-oxidant function. Front. Plant Sci. 6 (2015) 1147.
[21] Q. Yu, K. Feilke, A. Krieger-Liszkay, P. Beyer, Functional and molecular characterization of plastid terminal oxidase from rice (Oryza sativa). Biochim. Biophys. Acta 1837 (2014) 1284−1292.

[22] M.Trouillard, M. Shahbazi, L. Moyet, F. Rappaport, P. Joliot, M. Kuntz, G. Finazzi, Kinetic properties and physiological role of the plastoquinone terminal oxidase (PTOX) in a vascular plant. Biochim. Biophys. Acta 1817 (2012) 2140−2148.
[23] G. Ananyev, G. Renger, U. Wacker, V. Klimov, The photoproduction of superoxide radicals and the superoxide dismutase activity of Photosystem II. The possible involvement of cytochrome b559. Photosynth. Res. 41 (1994) 327−338.
[24] P. Pospíšil, A. Arató, A. Krieger-Liszkay, A. W. Rutherford, Hydroxyl radical generation by photosystem II. Biochemistry 43 (2004) 6783−6792.
[25] P. Pospíšil, I. Snyrychová, J. Kruk, K. Strzałka, J. Naus, Evidence that cytochrome b559 is involved in superoxide production in photosystem II: effect of synthetic short-chain plastoquinones in a cytochrome b559 tobacco mutant. Biochem. J. 397 (2006) 321−327.
[26] J. Kruk, K. Strzałka, Dark reoxidation of the plastoquinone-pool is mediated by the low-potential form of Cytochrome b-559 in spinach thylakoids. Photosynth. Res. 62 (1999) 273–279.
[27] P. Pospíšil, Enzymatic function of cytochrome b559 in photosystem II. J. Photochem. Photobiol. B. 104 (2011) 341−347.
[28] J. Kruk, M. Jemioła-Rzemińska, K. Burda, G.H. Schmid, K. Strzałka, Scavenging of superoxide generated in photosystem I by plastoquinol and other prenyllipids in thylakoid membranes, Biochemistry 42 (2003) 8501–8505.
[29] M. Kozuleva, I. Klenina, I. Proskuryakov, I. Kirilyuk, B. Ivanov, Production of superoxide in chloroplast thylakoid membranes ESR study with cyclic hydroxylamines of different lipophilicity, FEBS Letters 585 (2011) 1067–1071.
[30] D.K. Yadav, J. Kruk, R.K. Sinha, P. Pospíšil, Singlet oxygen scavenging activity of plastoquinol in Photosystem II of higher plants: electron paramagnetic resonance spin-trapping study. Biochim. Biophys. Acta 1797 (2010) 1807–1811.
[31] J. Kruk, A. Trebst, Plastoquinol as a singlet oxygen scavenger in Photosystem II. Biochim. Biophys. Acta 1777 (2008) 154–162.
[32] B. Nowicka, J. Kruk, Plastoquinol is more active than α-tocopherol in singlet oxygen scavenging during high light stress of *Chlamydomonas reinhardtii*. Biochim. Biophys. Acta 1817 (2012) 389–394.
[33] J. Kruk, R. Szymańska, Singlet oxygen and non-photochemical quenching contribute to oxidation of the plastoquinone-pool under high light stress in Arabidopsis. Biochim. Biophys. Acta 1817 (2012) 705–710.
[34] S.A. Khorobrykh, M. Karonen, E. Tyystjärvi, Experimental evidence suggesting that H_2O_2 is produced within the thylakoid membrane in a reaction between plastoquinol and singlet oxygen. FEBS Lett. 589 (2015) 779–786.
[35] M. Mubarakshina, S. Khorobrykh, B. Ivanov, Oxygen reduction in chloroplast thylakoids results in production of hydrogen peroxide inside the membrane. Biochim. Biophys. Acta 1757 (2006) 1496-1503.
[36] C. Bucke, R.M. Leech, M. Hallaway, R.A. Morton, The taxonomic distribution of plastoquinone and tocopherolquinone and their intracellular distribution in leaves of Vicia faba L. Biochim. Biophys. Acta 112 (1966) 19–34.
[37] J. Kruk, S. Karpinski, An HPLC-based method of estimation of the total redox state of plastoquinone in chloroplasts, the size of the photochemically active plastoquinone-pool and its redox state in thylakoids of Arabidopsis. Biochim. Biophys. Acta 1757 (2006) 1669–1675.
[38] G. K. Schweitzer, L. L. Pesterfield, The Aqueous Chemistry of the Elements. Oxford University Press: New York. (2010). 434.
[39] E. Tyystjärvi, S. Rantamäki, J. Tyystjärvi, Connectivity of Photosystem II is the physical basis of retrapping in photosynthetic thermoluminescence. Biophys. J. (2009) 96, 3735–3743.
[40] T. Sato, Y. Hamada, M. Sumikawa, S. Araki, H. Yamamoto, Solubility of oxygen in organic solvents and calculation of the hansen solubility parameters of oxygen. Ind. Eng. Chem. Res. 53 (2014) 19331–19337.

[41] P.S. Rao, E. Hayon, Redox potentials of free radicals. IV. Superoxide and hydroperoxy radicals $O_2^{\bullet-}$ and $HO_2^{\bullet}$. J. Phys. Chem. 79 (1975) 397–402.
[42] G. Hauska, E. Hurt, N. Gabellini, W. Lockau, Comparative aspects of quinol-Cytochrome c/plastocyanin oxidoreductases. Biochim. Biophys. Acta 726 (1983) 97–133.
[43] P.R. Rich, D.S. Bendall, The kinetics and thermodynamics of the reduction of Cytochrome c by substituted p-benzoquinols in solution. Biochim. Biophys. Acta 592 (1980) 506–518.
[44] J. Tokunaga, Solubilities of oxygen, nitrogen, and carbon dioxide in aqueous alcohol solutions. J. Chem. Eng. Data 20 (1975) 41–46.
[45] P. Mitchell, Possible molecular mechanisms of the protonmotive function of Cytochrome systems. J. Theor. Biol. 62 (1976) 327–367.
[46] Y. Song, G.R. Buettner, Thermodynamic and kinetic considerations for the reaction of semiquinone radicals to form superoxide and hydrogen peroxide. Free Radic. Biol. Med. 49 (2010) 919–962.
[47] R.C. Prince, P. L. Dutton, J. M. Bruce, Electrochemistry of ubiquinones: Menaquinones and plastoquinones in aprotic solvents. FEBS Lett. 160 (1983) 273–276.
[48] P. Wardman, Bioreductive activation of quinones: redox properties and thiol reactivity. Free Radic. Res. Communs. 8 (1990) 219–229.
[49] I.B. Afanas'ev, Superoxide ion: chemistry and biological implications. — CRC Press, Boca Raton, Florida, USA. (1989).
[50] D.T. Sawyer, J.L. Roberts Jr., Hydroxide ion: an effective one-electron reducing agent? Acc. Chem. Res. 21 (1988) 469–476.
[51] M.E. Peover, B.S. White, Electrolytic reduction of oxygen in aprotic solvents: The superoxide ion, Electrochimica Acta 11 (1966) 1061−1067
[52] M. Aguilar-Martínez, N. Macías-Ruvalcaba, I. González, Traveling through the square mechanism of the quinone reduction pathways. Influence of the proton donor addition on the reaction intermediaries in a non-aqueous solvent. Rev. Soc. Quím. Méx. 44 (2000) 74−81.
[53] X.Q. Zhu, C.H. Wang, H. Liang, Scales of oxidation potentials, pK(a), and BDE of various hydroquinones and catechols in DMSO. J. Org. Chem. 75 (2010) 7240-7257.
[54] S. Fukuzumi, T. Yorisue, Quinone/hydroxide ion induced oxygenation of p-benzoquinone to rhodizonate dianion ($C_6O_6^{2-}$) accompanied by one-electron reduction to semiquinone radical anion. J. Am. Chem. Soc. 113 (1991) 7764–7765.
[55] E. Lee-Ruff, A.B.P. Lever, J. Rigaudy, The reaction of catechol and derivatives with potassium superoxide Can. J. Chem. 54 (1976) 1837-1839.
[56] D. Vasudevan, H. Wendt**,** Electroreduction of oxygen in aprotic media. J. Electroanal. Chem. 192 (1995) 69-74.
[57] I.B. Afanas'ev, V.V. Grabovetskii, N.S. Kuprianova, Kinetics and mechanism of the reactions of superoxide ion in solution. Part 5. Kinetics and mechanism of the interaction of superoxide ion with vitamin E and ascorbic acid. J. Chem. Soc. Perkin Trans. 2 (1987) 281–285.
[58] Å. M. Leere Øiestad, A.C. Petersen, V. Bakken, J.Vedde, E. Uggerud, The oxidative power of protonated hydrogen peroxide. Angew. Chem. Int. Ed. 40 (2001) 1305–1309.
[59] P.Valtazanos, E.D. Simandiras, C.A. Nicolaides, Structure and vibrational analysis of protonated hydrogen peroxide. Chem. Phys. Letters 156 (1989) 240–244.
[60] Deepak Kumar Yadav, 1 Ankush Prasad, 1 Jerzy Kruk, 2 and Pavel Pospíšil Evidence for the involvement of loosely bound plastosemiquinones in superoxide anion radical production in photosystem II. PLoS One 9(12) (2014): e115466.
[61] J. Kruk, K. Strzalka, Redox changes of Cytochrome b(559) in the presence of plastoquinones. J. Biol. Chem. 276 (2001) 86–91.

[62] O.P.Kaminskaya, V.A. Shuvalov, Biphasic reduction of Cytochrome b_{559} by plastoquinol in photosystem II membrane fragments: evidence for two types of Cytochrome b_{559}/plastoquinone redox equilibria. Biochim. Biophys. Acta 1827 (2013) 471–483.
[63] D.W. Lawlor Photosynthesis: metabolism, control and physiology. Wiley, New York (1987)
[64] S. Caffarri, T. Tibiletti, R.C. Jennings, S. Santabarbara, A comparison between plant Photosystem I and Photosystem II architecture and functioning. Curr. Protein Pept. Sci. 15 (2014) 296–331.
[65] D. Takagi, S. Takumi, M. Hashiguchi, T. Sejima, C. Miyake, Superoxide and singlet oxygen produced within the thylakoid membranes both cause Photosystem I photoinhibition. Plant Physiol. 171 (2016) 1626–1634.
[66] R. Curci, J.O. Edwards, Activation of hydrogen peroxide by organic compounds. In *Catalytic oxidations with hydrogen peroxide as oxidant* (Strukul, G., Ed.) In the series Catalysis by metal complexes, Vol. 9, Chapter 2, Springer-Verlag LLC, New York (1992).
[67] V.V. Ptushenko, D.A. Cherepanov, L.I. Krishtalik, A.Y. Semenov, Semi-continuum electrostatic calculations of redox potentials in photosystem I. Photosynth Res. 97 (2008) 55–74.
[68] P. Sanchez-Cruz, A. Santos, S. Diaz, A.E. Alegría, Metal-independent reduction of hydrogen peroxide by semiquinones. Chem. Res. Toxicol. 27 (2014) 1380−1386.

Figure legends

Figure 1. Oxidation of PQH_2-9 in different organic mixtures. (A) In methanol; (B) in a mixture of methanol and 50 mM Mes-KOH, pH 5.0; (C) in methanol:50 mM Hepes-KOH, pH 8.0; (D) in hexane; (E) in hexane:50 mM Mes-KOH, pH 5.0; (F) in hexane:50 mM Hepes-KOH pH 8.0. The ratio between organic solvent and buffer was 1:1 (v:v).

Figure 2. Oxidation of PQH_2-9 in methanol upon addition of 1 mM KOH. 10 µl of 100 mM aqueous solution of KOH in was added to 1 ml of PQH_2-9 solution in methanol. The oxidation of PQH_2-9 was measured as decrease of fluorescence using excitation at 290 nm and emission at 330 nm (slit width 2 nm).

Figure 3. Dependence of PQH_2-9 oxidation and formation of PQ-9 and PQ-9-derived products on the concentration of KOH. 5 µl of KOH in aqueous solution was added to 60 µl of PQH_2-9 or PQ-9 solution, incubated for 2 minutes at 25 °C in the dark and then used for HPLC analysis. PQ-9-derived products are indicated as retention times of the corresponding peaks.

Figure 4. Kinetic curves of PQH_2-9 oxidation upon addition of different concentrations of KO_2 in DMSO to PQH_2-9 solution in acetonitrile. The measurements were performed with a stopped-flow instrument.

Figure 5. Dependence of the second order rate constant of oxidation of PQH_2-9 by KO_2 on the concentration of KO_2.

Figure 6. Dependence of PQH_2-9 oxidation and formation of PQ-9 and PQ-9-derived products on the concentration of KO_2. 10 µl of KO_2 in DMSO was added to 60 µl of PQH_2-9 (A, C) or PQ-9 (B, D) in acetonitrile, incubated for 2 minutes at 25 °C in the dark and then used for HPLC analysis.

Figure 7. Dependence of PQH_2-9 oxidation and formation of PQ-9 on the concentration of H_2O_2. 5 µl of aqueous solution of H_2O_2 was added to 60 µl of PQH_2-9 or PQ-9 solution in methanol, incubated for 2 and 40 minutes at 25 °C in the dark and then used for HPLC analysis.

Figure 8. Mechanisms of Cyt b_{559} mediated oxidation of PQH_2-9 associated with formation $O_2^{\bullet-}/HO_2^{\bullet}$ and H_2O_2 within the thylakoid membrane. Reactions of phase A yield $O_2^{\bullet-}$ or $HO_2^{\bullet}$ and reactions of phase B result in oxidation of both reduced Cyt b_{559} and PQH_2-9 by $O_2^{\bullet-}$. Formation of Cyt b_{559}[$(H^+)PQH^{\bullet}$-9] complex in a reaction of Cyt b_{559} with PQH_2-9 (Reaction I). Decomposition of the complex via Reaction II or in a reaction with PQ-9 (Reaction III) produces the reduced state of Cyt b_{559} (Cyt b_{559}^{red}), H^+ and $PQH^{\bullet}$-9. Oxidation of $PQH^{\bullet}$-9 by O_2 to form $HO_2^{\bullet}$ (Reaction IV). Deprotonation of $PQH^{\bullet}$-9 (Reaction V). Oxidation of $PQ^{\bullet-}$-9 by O_2 to form $O_2^{\bullet-}$ (Reaction VI). Reduction of PQ-9 (Reaction VII) and reduction of O_2 (Reaction VIII) by Cyt b_{559}^{red}. Reduction of $O_2^{\bullet-}$ (Reactions IX and XI) and $HO_2^{\bullet}$ (Reactions X and XII) by PQH_2-9 and by Cyt b_{559}^{red}, respectively.

Figure 9. Summary of the mechanisms of production and scavenging of ROS in the thylakoid membrane. Reduction of O_2 by $PQ^{\bullet-}$-9 or $PQH^{\bullet}$-9 (Reaction 1). Reduction of O_2 by PQH_2-9 in a series of reactions mediated by Cyt b_{559} (Reaction 2). Oxidation of PQH_2-9 by $^1O_2$ (Reaction 3). Reduction of $O_2^{\bullet-}$ by PQH_2 (Reaction 4). Reduction of H_2O_2 by PQH_2-9 (Reaction 5). Formation of H_2O_2 in a series of reactions mediated by Cyt b_6/f (Reaction 6). Formation of $O_2^{\bullet-}$ at phylloquinone A1 of PSI (Reaction 7) and it reduction by PQH_2 (Reaction 4). Formation of $HO^{\bullet}$ by reduction of H_2O_2 by phylloquinone A1 and iron-sulfur centers of PSI (Reaction 8). PTOX mediated formation of $O_2^{\bullet-}$: reduction of oxygen at the catalytic non-heme diiron center of PTOX (Reaction 9), formation of $PQH^{\bullet}$-9 which can be deprotonated and then oxidized by O_2 (Reaction 10). Mehler-peroxidase reaction: reduction of O_2 by iron-sulfur centers of PSI (Reaction 11), dismutation of $O_2^{\bullet-}$ (Reaction 12) and detoxification of H_2O_2 (Reaction 13).

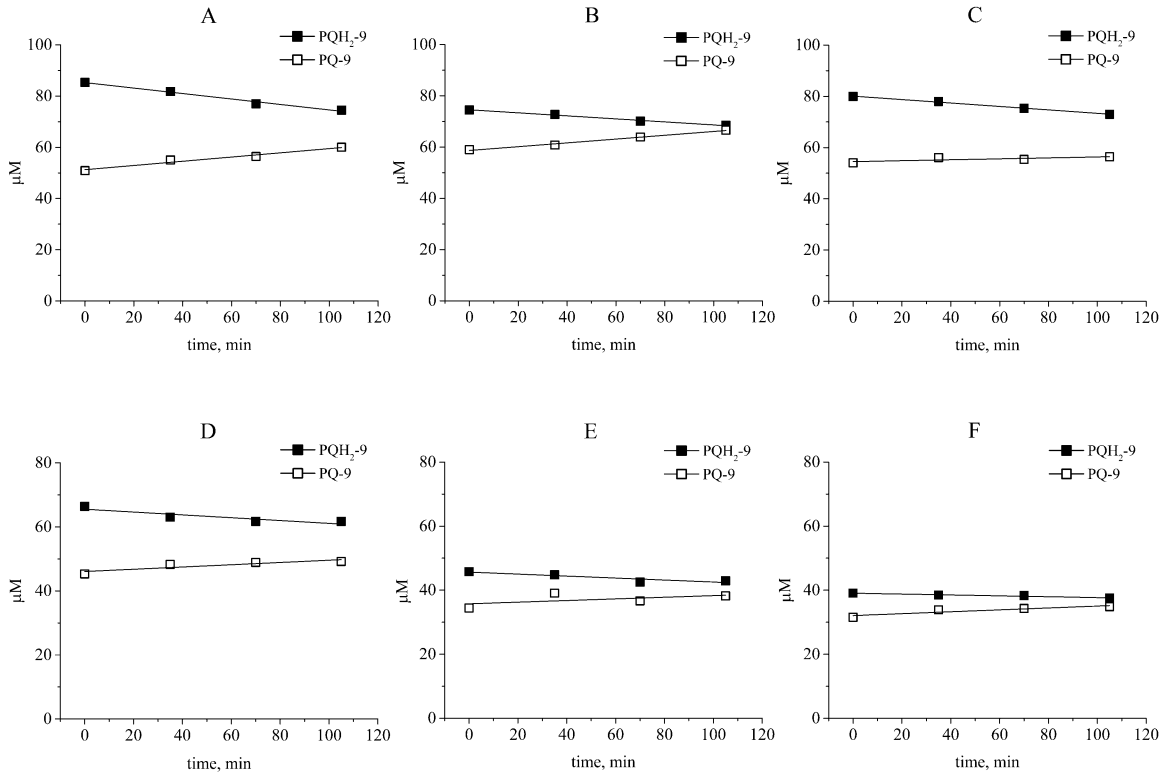

Fig. 1.

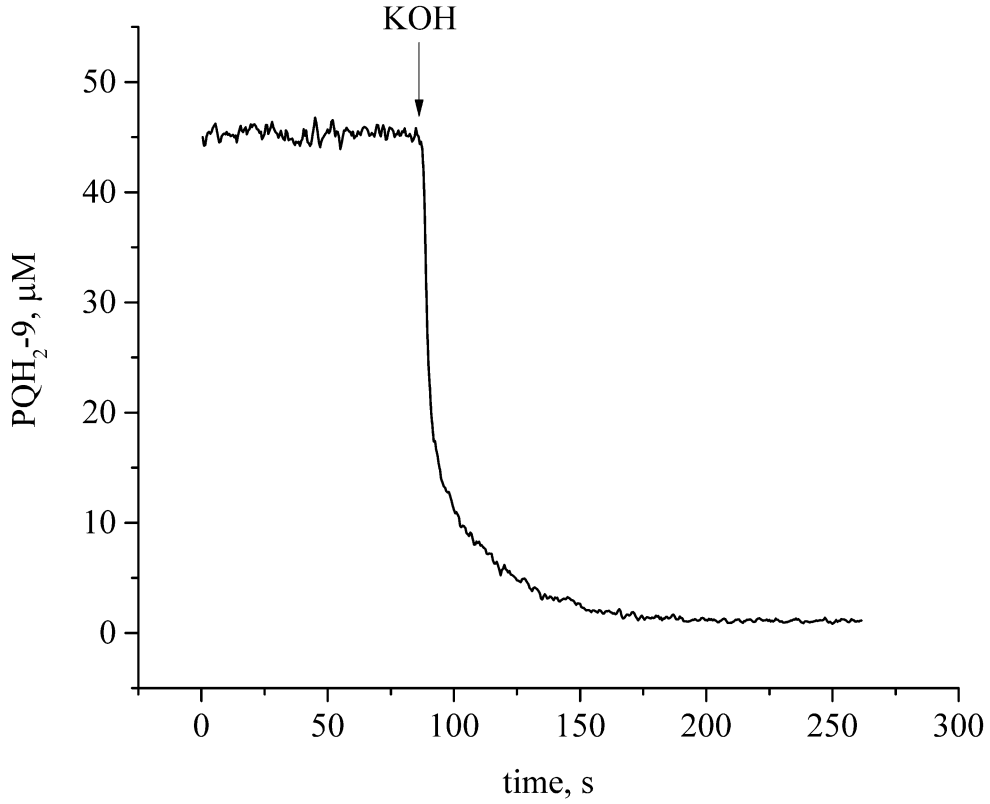

Fig. 2.

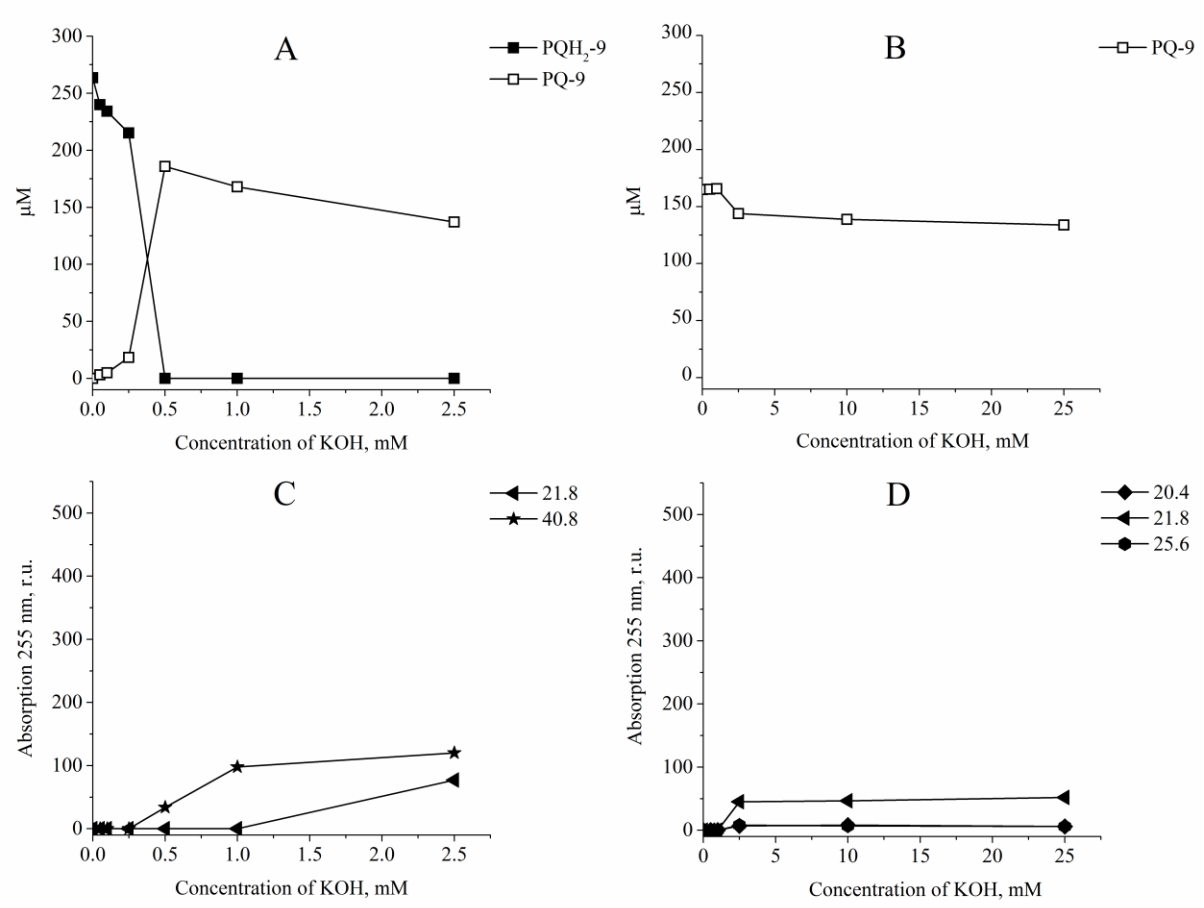
A
PQH2-9
PQ-9
μM
Concentration of KOH, mM
B
PQ-9
μM
Concentration of KOH, mM
C
21.8
40.8
Absorption 255 nm, r.u.
Concentration of KOH, mM
D
20.4
21.8
25.6
Absorption 255 nm, r.u.
Concentration of KOH, mM

Fig. 3.

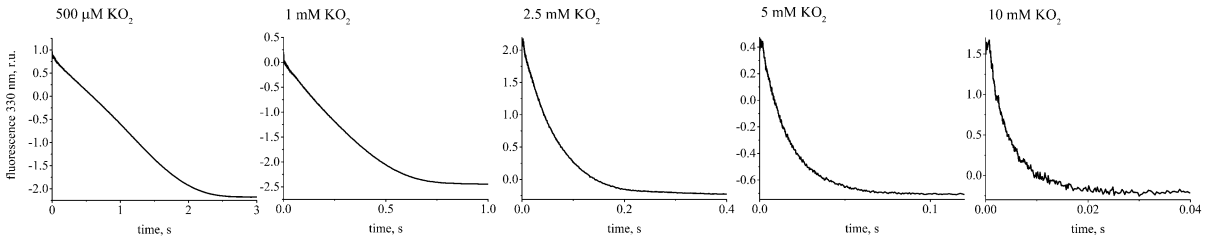
500 μM KO2
1 mM KO2
2.5 mM KO2
5 mM KO2
10 mM KO2
fluorescence 330 nm, r.u.
time, s

Fig. 4.

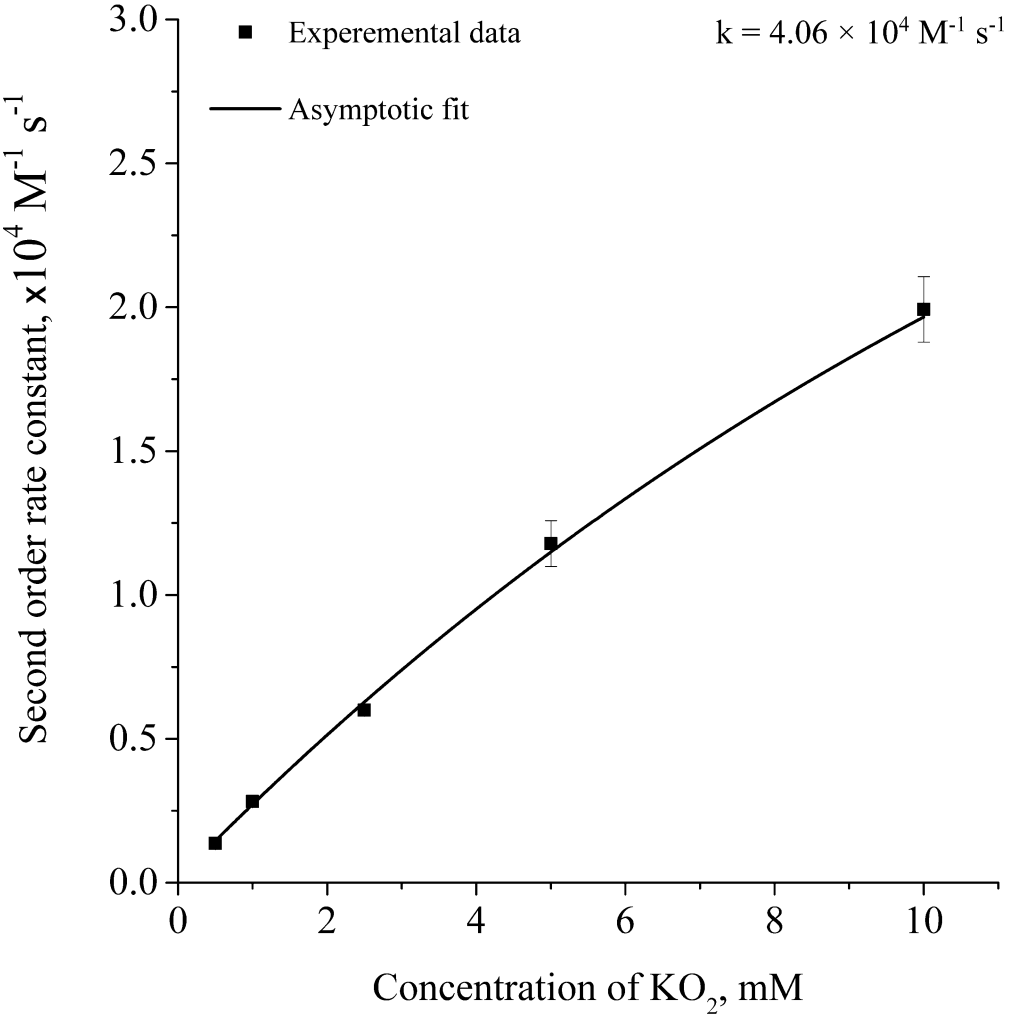
Experemental data
k = 4.06 × 10^4 M^-1 s^-1
Asymptotic fit
Second order rate constant, x10^4 M^-1 s^-1
Concentration of KO2, mM
3.0
2.5
2.0
1.5
1.0
0.5
0.0
0
2
4
6
8
10

Fig. 5.

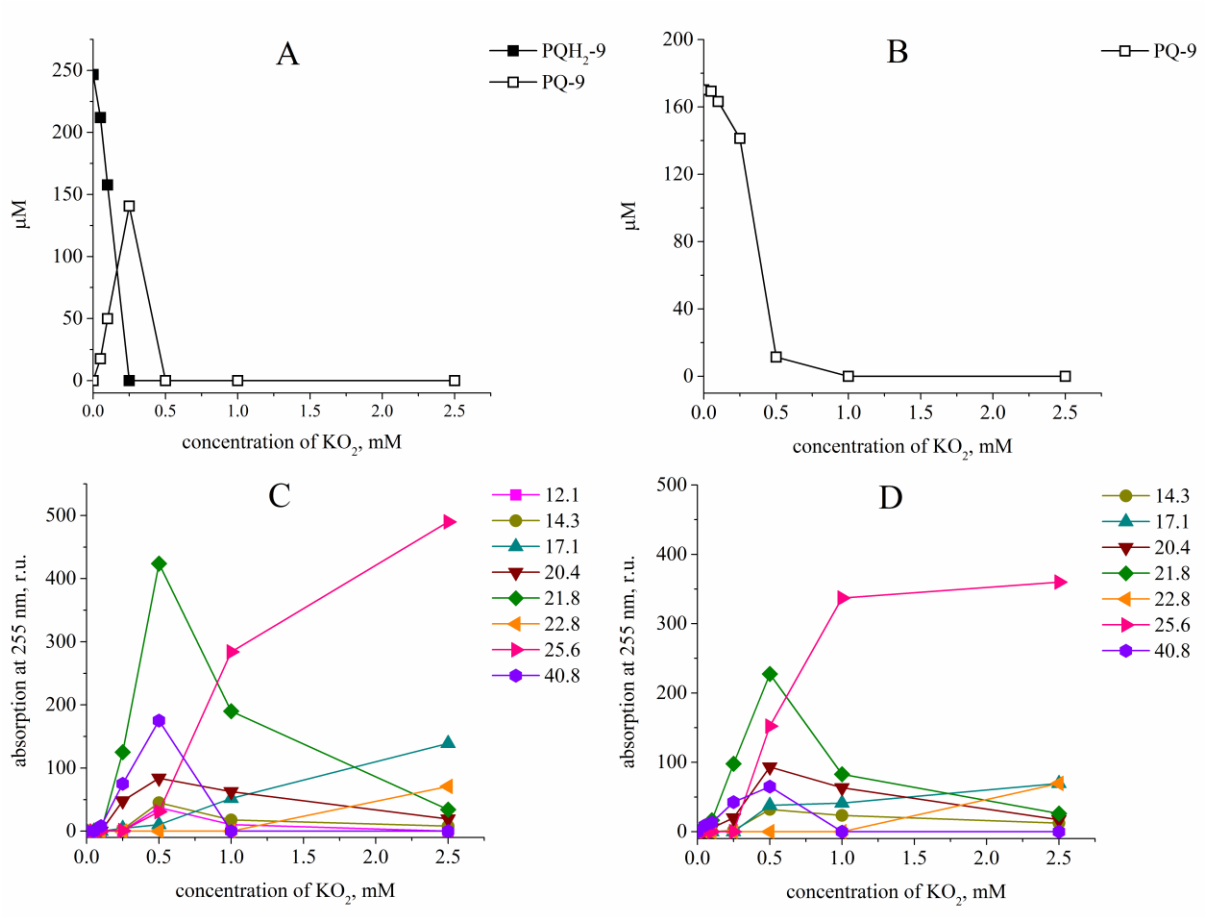
A
PQH2-9
PQ-9
µM
concentration of KO2, mM
B
PQ-9
µM
concentration of KO2, mM
C
12.1
14.3
17.1
20.4
21.8
22.8
25.6
40.8
absorption at 255 nm, r.u.
concentration of KO2, mM
D
14.3
17.1
20.4
21.8
22.8
25.6
40.8
absorption at 255 nm, r.u.
concentration of KO2, mM

Fig. 6

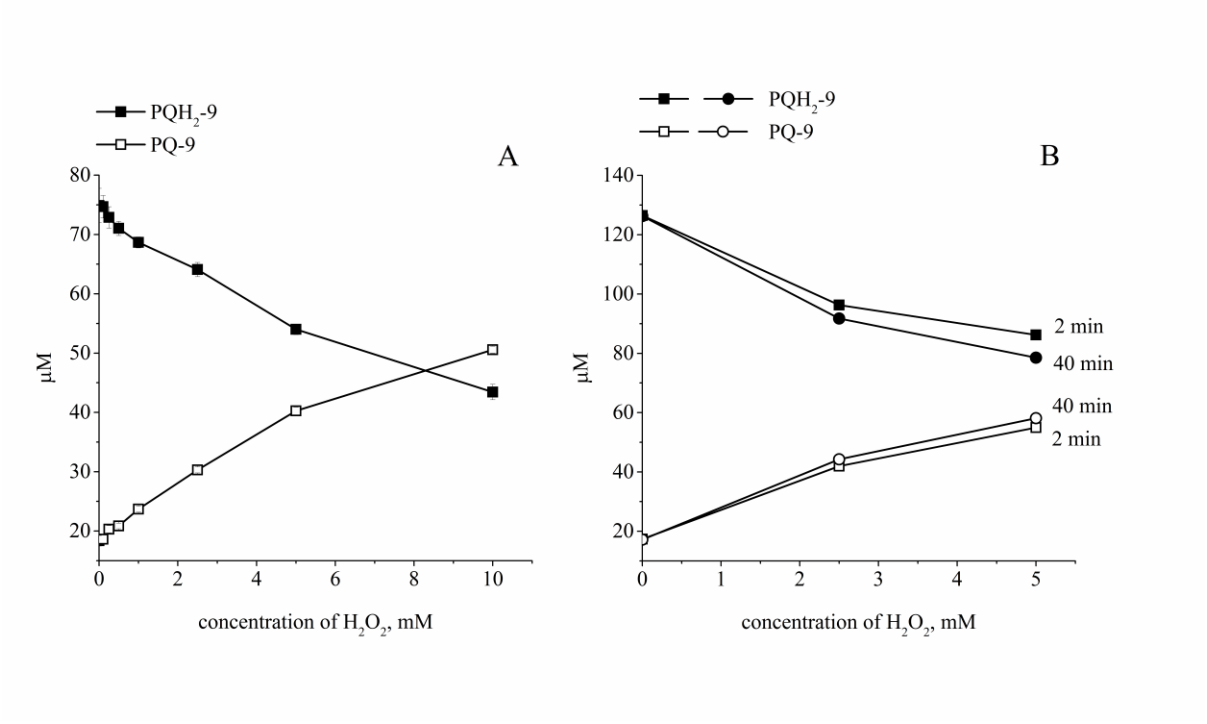
PQH2-9
PQ-9
A
μM
concentration of H2O2, mM
PQH2-9
PQ-9
B
2 min
40 min
40 min
2 min
μM
concentration of H2O2, mM

Fig. 7

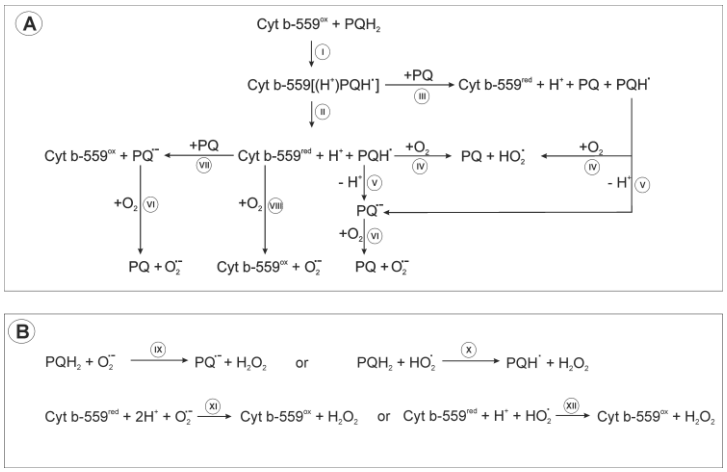
A
Cyt b-559ox + PQH2
I
Cyt b-559[(H+)PQH•]
+PQ
III
Cyt b-559red + H+ + PQ + PQH•
II
Cyt b-559ox + PQ•−
+PQ
VII
Cyt b-559red + H+ + PQH•
+O2
IV
PQ + HO2•
+O2
IV
- H+
V
- H+
V
+O2
VI
+O2
VIII
PQ•−
+O2
VI
PQ + O2•−
Cyt b-559ox + O2•−
PQ + O2•−
B
PQH2 + O2•−
IX
PQ•− + H2O2
or
PQH2 + HO2•
X
PQH• + H2O2
Cyt b-559red + 2H+ + O2•−
XI
Cyt b-559ox + H2O2
or
Cyt b-559red + H+ + HO2•
XII
Cyt b-559ox + H2O2

Fig. 8

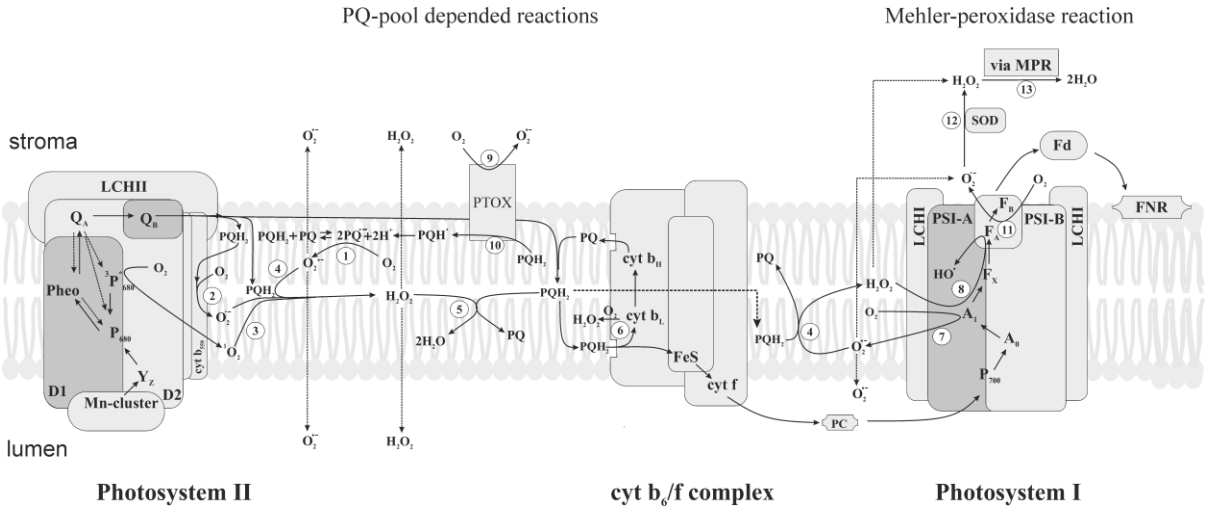
PQ-pool depended reactions
Mehler-peroxidase reaction
stroma
lumen
LCHII
PTOX
via MPR
SOD
Fd
FNR
PSI-A
PSI-B
LCHI
Pheo
D1
D2
Mn-cluster
cyt b$_H$
cyt b$_L$
FeS
cyt f
PC
Photosystem II
cyt b$_6$/f complex
Photosystem I

Fig. 9

Table 1. The second order rate constant of oxidation of PQH_2-9 by O_2 in pure methanol, hexane, methanol-buffer and hexane-buffer solutions containing PQ-9 at 25 ˚C in the dark. The concentration of O_2 in methanol was taken as 2.42 mM and for methanol:buffer solutions, the concentration of O_2 was assumed to be the same as for methanol:water 471 µM [36]. The rate constants of PQH_2-9 oxidation for hexane and hexane:buffer systems was calculated using the O_2 concentration of 3.58 mM for hexane and 256 µM for the hexane-buffer system assuming that oxidation of PQH_2-9 can occur both within the hexane phase and at the interface between hexane and the buffer.

Composition of medium	Second order rate constant of PQH_2-9 oxidation, M^{-1} s^{-1}		
	Methanol	Hexane	Hexane-buffer interface
Pure solvent	7.85×10^{-3}	4.71×10^{-3}	
Solvent plus 50 mM Mes-KOH, pH 5.0 (1:1, v/v)	2.96×10^{-2}	4.73×10^{-3}	6.62×10^{-2}
Solvent plus 50 mM Hepes-KOH, pH 8.0 (1:1, v/v)	2.92×10^{-2}	1.29×10^{-3}	1.81×10^{-2}

Table 2. Second order rate constant of PQH_2-9 oxidation and the rate of oxidation of PQH_2-9 inside and on the surface of the thylakoid membrane. The following values were used for the calculations: volume of chloroplast, 3.6×10^{-5} L (mg Chl)$^{-1}$ [55]; volume of thylakoid membrane, 4.6×10^{-6} L (mg Chl)$^{-1}$ [55]; molar mass of chlorophyll – 894 g mol^{-1} from [55]; amount of low potential form of cyt b_{559} – 0.3×10^{-3} mol (mol Chl)$^{-1}$ from [23]; amount of photoactive PQH_2-9 in thylakoids – 14×10^{-3} mol (mol Chl)$^{-1}$ [23]; concentration of oxygen inside and outside of thylakoid membrane, 2.4 mM and 253 µM, respectively [23]. The ratio between both PSI:Chl was taken as 1:420 [56]. The ratio of Cyt b_6/f complex to PS I was taken as 1:1. The rates and second order rate constants for oxidation were calculated assuming even distribution of PSI, PQH_2-9, Cyt b_{559} and Cyt b_6/f in volume of stroma (for membrane surface) and volume of thylakoid membrane (for membrane).

Conditions	Second order rate constant, M^{-1} s^{-1}	Rate of oxidation, M s^{-1}
PQH_2-9 oxidation in membrane in the dark after photoreduction[3]	6.3	5.14×10^{-5}
PQH_2-9 oxidation on membrane surface in the dark after photoreduction[3]	63	7.94×10^{-6}
PQH_2-9 oxidation in membrane in the light (from O_2 consumption[2] at PPDF 30 – 500 µmol m^{-2} s^{-1})	1.48×10^{2}	1.21×10^{-3}
PQH_2-9 oxidation on membrane surface in the light (from O_2 consumption[2] at PPDF 30 – 500 µmol m^{-2} s^{-1})	1.43×10^{3}	1.8×10^{-4}
Oxidation of PQH_2-9 in membrane via dismutation[1]	1.29×10^{-3}	1.05×10^{-8}
Oxidation of PQH_2-9 on membrane surface via dismutation[1]	1.81×10^{-2}	2.28×10^{-9}
Oxidation of Cyt b_{559}LP by O_2 in membrane in the dark[3]	5.5	9.64×10^{-7}
Oxidation of Cyt b_{559}LP by O_2 on the lumenal side of thylakoid membrane in the dark[3]	55	1.47×10^{-7}
Oxidation of PSI by O_2 in membrane (from oxygen consumption)[4]	7.25×10^{2}	9×10^{-4}
Oxidation of PSI by O_2 on stromal side (from oxygen consumption)[4]	6.07×10^{3}	1.3×10^{-4}

Oxidation of Cyt b_6/f by O_2 in membrane[5]	5.07×10^{2}	6.3×10^{-4}
Oxidation of Cyt b_6/f by O_2 on the stromal side[5]	4.29×10^{3}	9.2×10^{-5}
PTOX-mediated oxidation of PQH_2-9 by O_2 in membrane[6]	10.6	8.68×10^{-5}
PTOX-mediated oxidation of PQH_2-9 by O_2 on the stromal side[6]	1.01×10^{2}	1.27×10^{-5}
PTOX-mediated oxidation of PQH_2-9 associated with H_2O_2 production in membrane[7]	1.8	1.47×10^{-5}
PTOX-mediated oxidation of PQH_2-9 associated with H_2O_2 on the stromal side[7]	17	2.16×10^{-6}

[1]The rate of PQH_2-9 oxidation was calculated using the second order rate constant of PQH_2-9 oxidation in a hexane:buffer system at pH 8.0. [2]The rate of PQH_2-9 oxidation was calculated from the rate of oxygen consumption associated with PQH_2-9 oxidation [17]. [3]The rates of PQH_2-9 and Cyt b_{559} oxidation in thylakoids in the dark after photoreduction [23]. [4]The rate of PSI oxidation was calculated from the rate of oxygen consumption associated with PSI oxidation [16]. [5]The rate of Cyt b_6/f oxidation was calculated from the rate of superoxide generation associated with Cyt b_6/f [18]. [6]The rate of PTOX-mediated oxidation of PQH_2-9 was calculated from PQH_2-9 oxidation kinetics in tomato leaves where rate of electron transfer from PQH_2-9 to oxygen was evaluated to be 0.3 e^- $PSII^{-1}$ s^{-1} [22]. [7]The PTOX-mediated oxidation of PQH_2-9 associated with H_2O_2 production was calculated from PQH_2-9 oxidation kinetics in tomato leaves [22] assuming that the ROS production via PTOX-mediated oxidation of PQH_2-9 can reach 17% from total reduction of oxygen [21].

Supplementary information for Khorobrykh S, Tyystjärvi E: Plastoquione generates and scavenges reactive oxygen species in thylakoids

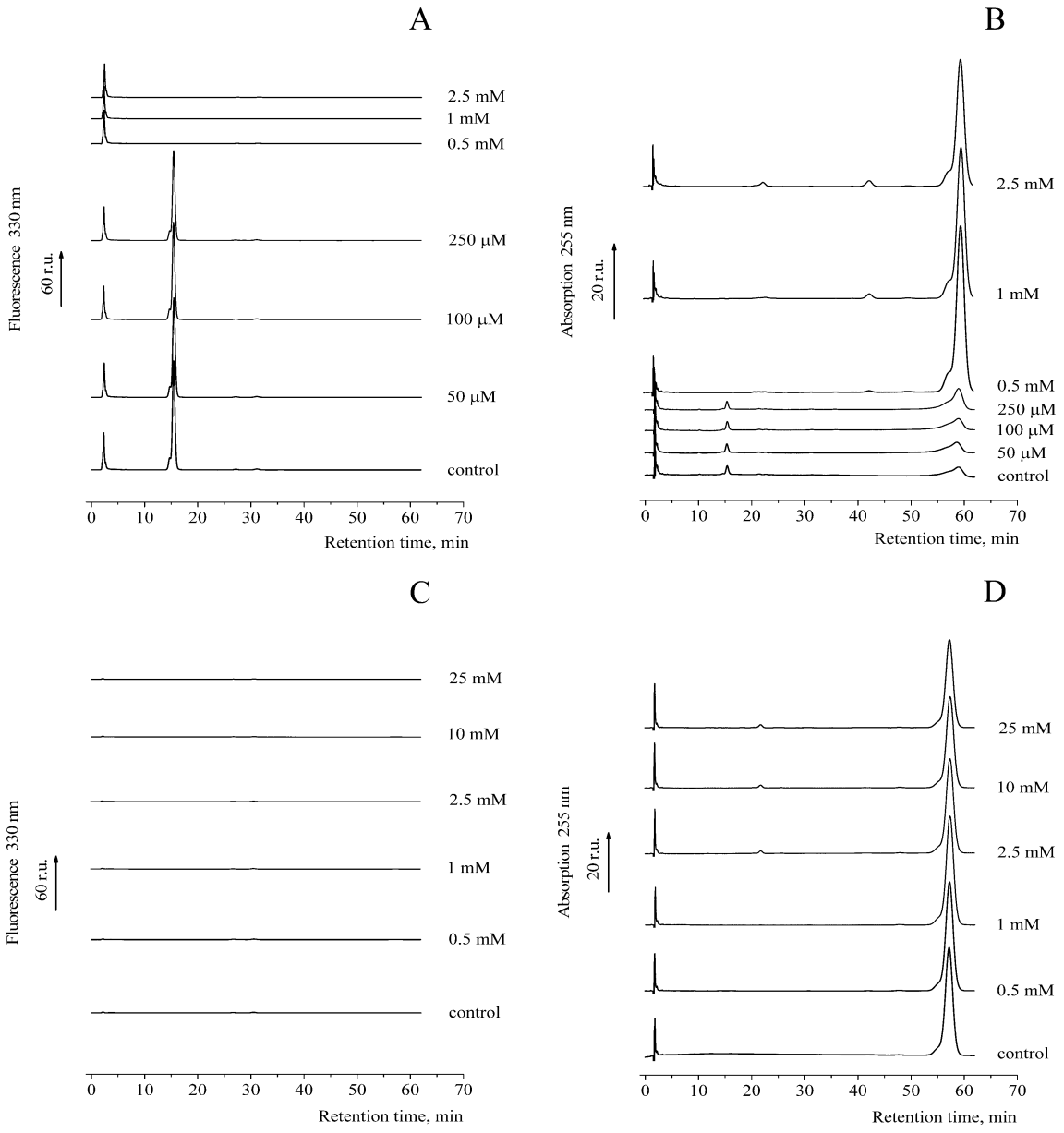

Figure S1. Typical chromatograms of PQ-9-derived products upon addition of aqueous solution of KOH to PQH_2-9 (A, B) and PQ-9 (C, D) solution in methanol. The chromatograms (A, C) were measured using fluorescence detection at excitation 290 nm and emission at 330 nm and chromatograms (B, D) were measured using absorption detection at 255 nm.

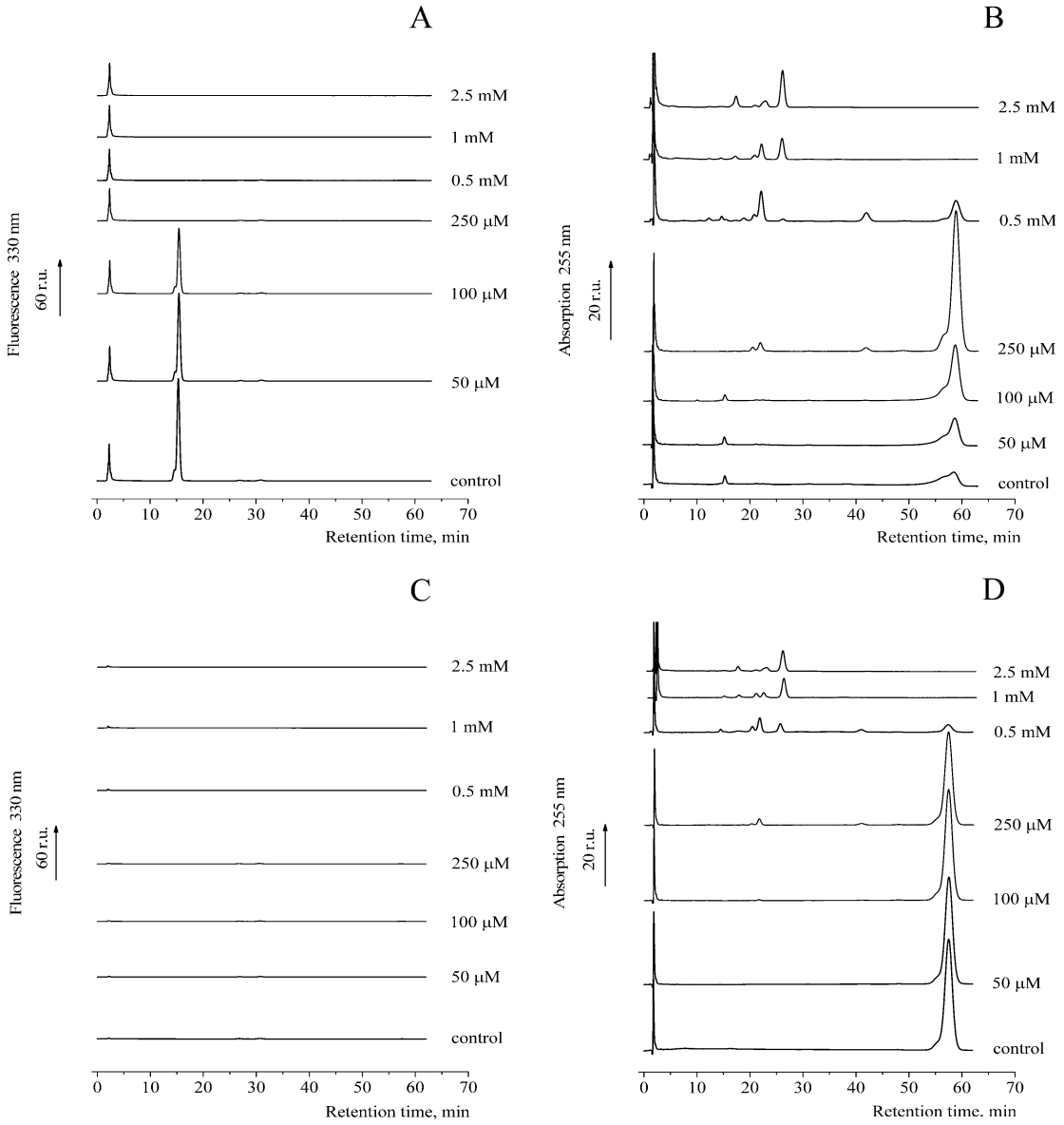

Figure S2. Typical chromatograms of PQ-9-derived products upon addition of KO_2 in dimethylsulfoxide to PQH_2-9 (A, B) and PQ-9 (C, D) solution in acetonitrile. The chromatograms (A, C) were measured using fluorescence detection at excitation 290 nm and emission at 330 nm and chromatograms (B, D) were measured using absorption detection at 255 nm.

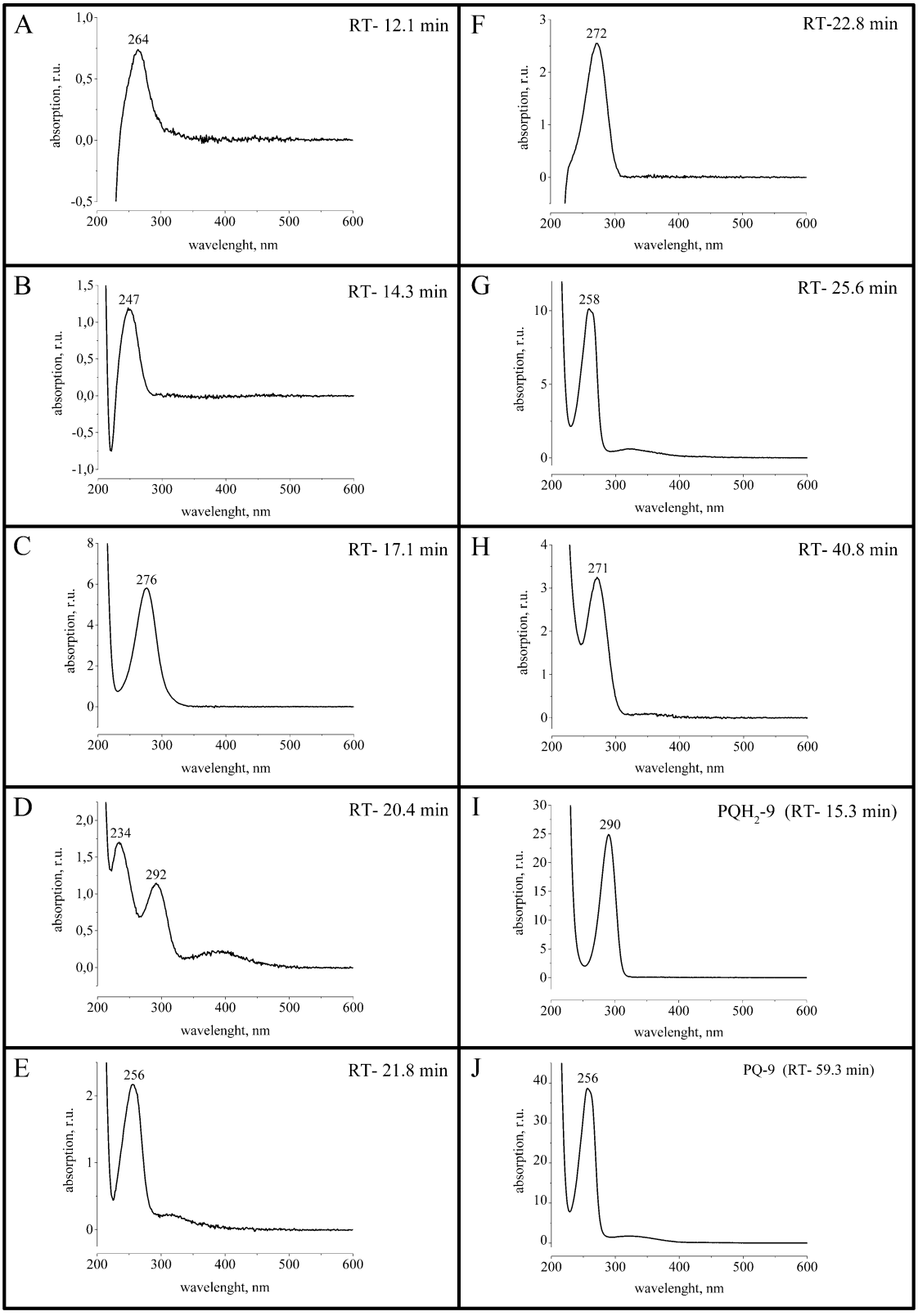

Figure S3. Absorption spectra of PQ-9 derivatives (A-H) and PQH_2-9 (I) and PQ-9 (J). PQ-9 derivatives are formed in the reactions of KO_2 or KOH with PQH_2-9 and PQ-9. The retention time of each compound is given in the upper right corner.

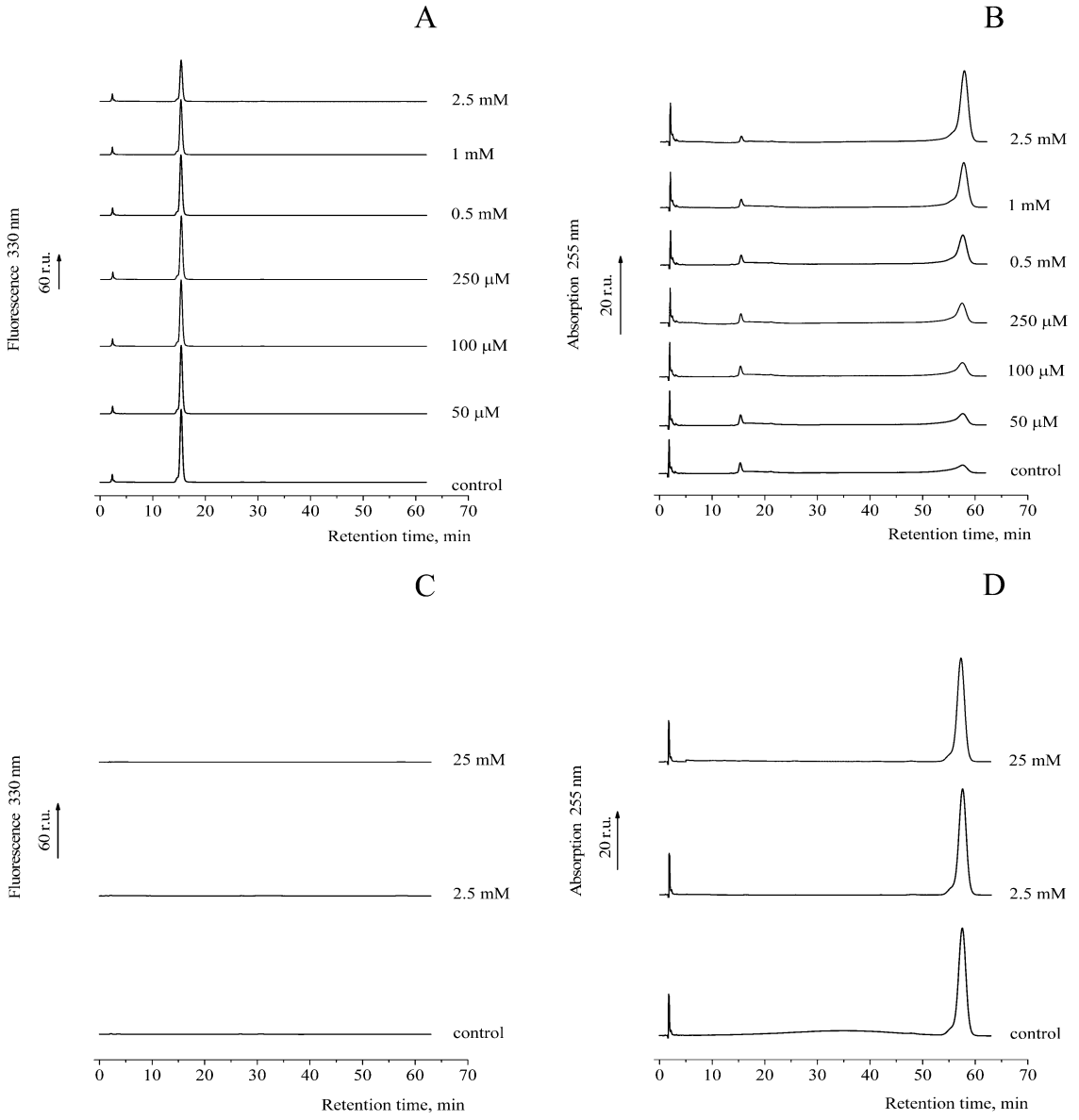

Figure S4. Typical chromatograms of PQ-9-derived products upon addition of aqueous solution of H_2O_2 to PQH_2-9 (A, B) and PQ-9 (C, D) solution in methanol. The chromatograms (A, C) were measured using fluorescence detection at excitation 290 nm and emission at 330 nm and chromatograms (B, D) were measured using absorption detection at 255 nm.